Complexity of waves in nonlinear disordered media

C. Conti[1,3,*] and L. Leuzzi[2,3,†]

[1]*ISC-CNR, UOS Roma, Piazzale A. Moro 2, I-00185, Roma, Italy*

[2]*IPCF-CNR, UOS Roma, Piazzale A. Moro 2, I-00185, Roma, Italy*

[3]*Dipartimento di Fisica, Università di Roma Sapienza, Piazzale A. Moro 2, I-00185, Roma, Italy*

(Received 16 September 2010; revised manuscript received 17 January 2011; published 18 April 2011)

The statistical properties of the phases of several modes nonlinearly coupled in a random system are investigated by means of a Hamiltonian model with disordered couplings. The regime in which the modes have a stationary distribution of their energies and in which the phases are coupled is studied for arbitrary degrees of randomness and energy. The complexity versus temperature and strength of nonlinearity is calculated. A phase diagram is derived in terms of the stored energy and amount of disorder. Implications in random lasing, nonlinear wave propagation, and finite-temperature Bose-Einstein condensation are discussed.

DOI: 10.1103/PhysRevB.83.134204 PACS number(s): 42.55.Zz, 42.60.Fc, 64.70.P–

The interplay between disorder and nonlinearity in wave propagation is a technically challenging process. Such a problem arises in several different frameworks in modern physics, such as nonlinear optical propagation and laser emission in random systems, Bose-Einstein condensation (BEC), and Anderson localization (as, e.g., in Refs. [1–24]). Related topics are the supercontinuum generation and condensation processes.[25–30]

When disorder has a leading role, nonlinear processes can be largely hampered due to the fact that waves rapidly diffuse in the system. Conversely, if the structural disorder is perturbative, its effect on nonlinear evolution is typically marginal, leading to some additional linear or nonlinear scattering losses, but not radically affecting the qualitative nonlinear regime expected in the absence of disorder. When disorder and nonlinearity play on the same ground, one can envisage novel and fascinating physical phenomena; however, the technical analysis is rather difficult, as the problem cannot be attacked by perturbational expansions.

Physically, disorder and nonlinearity compete in those regimes when wave scattering affects the degree of localization, eventually inducing it (as in the Anderson localization), and nonlinearity couples the modes in the system. These may in general exhibit a distribution of localization lengths (determined by the amount of disorder) and a strength of the interaction depending on the amount of energy coupled in the system. In this respect, the onset of localization when increasing the degree of disorder affects the nonlinear interaction by increasing the statistical spread of the coupling coefficients, due to the large variation of the overlap integrals [cf., e.g., Eqs. (8) and (26) in Secs. I A and I B] between modes with various spatial extensions.

Our interest here is to provide a general theoretical framework, whose result is the prediction of specific transitions from incoherent to coherent regimes, which are specifically due to the disorder and display a glassy character, associated with a large number of degenerate states present in the system.

We adopt a statistical mechanics perspective to the problem, which allows one to derive very general conclusions, not depending on the specific problem, and our focus is on the case in which many modes are excited. This implies that energy is distributed among many excitations in an initial stage of the dynamics. The overall coherence (i.e., the statistical properties of the overall wave) will be determined by the phase relations between the involved modes. Here we show that there exist collective disordered regimes, where coherence is dictated by the fact that the system is trapped in one of many energetically equivalent states, as described below.

Representing mode phases by means of continuous planar XY-like spins and applying a statistical mechanics approach we can identify different thermodynamic phases. For negligible nonlinearity, all the modes will oscillate independently in a continuous wave noisy regime ("paramagneticlike" phase). For a strong interaction and a suitable sign of the nonlinear coefficients, all the modes will oscillate coherently ("ferromagneticlike" regime). This corresponds, for example, to standard passively mode-locked laser systems,[31] which we found to take place even in the presence of a certain amount of disorder. In intermediate regimes, the tendency to oscillate synchronously will be frustrated by disorder, resulting in a glassy regime.

These three regimes are identified by a set of order parameters (up to ten for the most complicated phase, as detailed below), which can be cast into two classes: the "magnetizations" m and the "overlaps" q. As the system is in the paramagneticlike phase all m and q vanish; in the ferromagnetic regime they are both different from zero, while in the glassy phase $m = 0$ and (at least some of) the overlap parameters are different from zero.

The paramagnetic and ferromagnetic phases may be present even in the absence of disorder; conversely, a necessary condition to find a glassy phase is frustration (disorder induced in our case, see Sec. III A). The glassy phase is characterized by the occurrence of a rugged—complex—landscape for the Gibbs free energy functional in the mode phases space: a huge number of minima are present, corresponding to a multitude of stable and metastable states in the system, separated by barriers of various heights and clustered in basins. This is a result of the competition between disorder and nonlinearity.

The existence of a nonvanishing *complexity* (which measures the number of energetically equivalent states) for the possible distributions of mode phases is the basic ingredient for explaining a variety of novel phenomena like speckle pattern fluctuations and spectral statistics for disordered, or weakly disordered nonlinear, systems, ergodicity breaking, glassy transitions of light or BEC, and, ultimately, the onset

of a coherent regime in a random nonlinear system. Indeed, following known results from glassy physics, we expect that the dynamic phase transitions, predicted in this work by the mean-field approach, will result in experimentally observable effects such as diverging relaxation times and history-dependent responses.

Our work extends previously reported results, cf. Ref. 32, and it includes an arbitrary degree of disorder and the discussion of its application to nonlinear Schrödinger models, relevant, e.g., for BEC, spatial nonlinear optics, and supercontinuum generation.

The paper is organized as follows: in Sec. I we introduce the model and we discuss some of its possible fields of application, namely, random lasers, BECs, and optical propagation; in Sec. II we discuss the effect of disorder in the coupling of light modes and the new expected phenomena; we dedicate Sec. III to an extremely basic introduction to the statistical mechanics of systems with quenched disorder, to the replica method, and to the definition of complexity; in Sec. IV we study the model within the replica approach, details of the computation are reported in the Appendix; in Sec. V we discuss the presence of excited metastable states and we compute the complexity functional; in Sec. VI we show the phase diagrams of our model and discuss the properties of its thermodynamic phases; and in Sec. VII we draw our conclusions.

I. THE LEADING MODEL

Here we review some of the disordered systems where a relevant nonlinear interaction may arise and our model applies. The basic Hamiltonian of N adimensional angular variables $\phi \in [0 : 2\pi]$ is given by

$$\mathcal{H}_J[\phi] = -\sum_{\substack{i_1 < i_2, i_3 < i_4 \\ i_1 < i_3}}^{1,N} J_{\mathbf{i}} \cos(\phi_{i_1} + \phi_{i_2} - \phi_{i_3} - \phi_{i_4}), \quad (1)$$

where $\mathbf{i} = \{i_1, i_2, i_3, i_4\}$ and $J_{\mathbf{i}}$ are random independent identically distributed interaction variables. Formally, the couplings can vary from short to long range, depending on the structure of the four-index interaction tensor $J_{\mathbf{i}}$. If we choose $J_{\mathbf{i}} \neq 0$ for any distinct quadruple $i_1, \ldots, i_4$, independently of the geometric position, we can build a mean-field theory in which the system is fully connected. In this case the average $J_{\mathbf{i}}$ and the variance of its distribution must scale as $1/N^3$ to guarantee thermodynamic convergence of (free) energy density. The interaction can, otherwise, be bond-diluted with an arbitrary degree of diluteness, adopting a sparse tensor whose nonzero elements do not scale with the number of modes.

As we show in the following, the Hamiltonian, Eq. (1), is derived in different contexts, and the various parameters may have different interpretations. In this manuscript we want to derive general properties that are expected assuming a simple, yet reasonable, Gaussian distribution for the random coupling coefficients, with a nonvanishing mean value. Varying the ratio between the standard deviation and the mean value we control a different degree of disorder. Hence, these results apply to the various cases in which random wave propagation, localization, and not-negligible nonlinear effects are important; a few of them are detailed in the following.

As a thermodynamic approach is adopted, one can argue if the statistical mechanics techniques also apply in those systems where the definition of a temperature is not straightforward, as, specifically, nonlinear optical wave propagation in disordered media. This particular problem can, then, be treated as for constraint satisfaction problems in computer science,[33–36] where—at the end of the calculation—the limit of zero temperature is taken and it is shown that a transition is expected as the number of constraints grows.

As detailed in the next section, in the following we emphasize the nonlinear interaction of a discrete set of modes. This corresponds to the *strong cavity limit*, or to the case of a *closed cavity*. The presence of a continuous spectrum, corresponding to radiation modes, results in linear coupling terms that we will consider elsewhere. In addition, the considered set of interacting modes is not necessarily to be taken as complete: we just consider a subset of modes which is expected to be strongly interacting. The fact that for BEC the wave function can be expressed as a superposition of localized states has also been addressed in Refs. [2,3]. The role of the continuous spectrum has been also considered in Refs. [37–39].

A. Random active and passive electromagnetic cavities

We start from the electromagnetic energy inside a dielectric cavity (due to the generality of the considered model similar examples can be found in a variety of systems):

$$\mathcal{E}_{\mathrm{EM}} = \int \mathbf{E}(\boldsymbol{r}) \cdot \mathbf{D}(\boldsymbol{r})\, dV. \quad (2)$$

The displacement vector is written in terms of a position-dependent relative dielectric constant $\epsilon_r(\mathbf{r})$:

$$\mathbf{D}(\mathbf{r}) = \epsilon_0 \epsilon_r(\mathbf{r}) \mathbf{E}(\mathbf{r}) + \epsilon_0 \mathbf{P}_{\mathrm{NL}}(\mathbf{r}), \quad (3)$$

with $\mathbf{P}_{\mathrm{NL}}$ being the nonlinear polarization. In the absence of the latter, for a closed cavity, the field can be expanded in terms of the modes of the system. In the presence of disorder these modes may display a different degree of localization as, e.g., in a disordered photonic crystal (PhC).[40] For a closed cavity these modes form a complete set and the field can be expanded in terms of the modes

$$\mathbf{E} = \Re\left[\sum_{n=1}^{N} a_n(t) \exp(-\imath \omega_n t) \mathbf{E}_n(\mathbf{r})\right], \quad (4)$$

with $\mathbf{E} = \{E^x, E^y, E^z\}$. As far as a nonlinear polarization is not present, the coefficients a_n are time independent. Conversely, in the general case, taking for $\mathbf{P}_{\mathrm{NL}}$ a standard third-order expansion, one has for the nonlinear interaction Hamiltonian

$$\begin{aligned} \mathcal{H} &= -\left\langle \int \epsilon_0 \mathbf{E} \cdot \mathbf{P}_{\mathrm{NL}} dV \right\rangle \\ &= -\sum_{\omega_j + \omega_k = \omega_l + \omega_m} \Re[G_{jklm} a_j a_k a_l^* a_m^*], \end{aligned} \quad (5)$$

where $\langle \cdots \rangle$ is the time average over an optical cycle and the sum ranges over all distinct 4-ples for which the condition

$$\omega_j + \omega_k = \omega_l + \omega_m \quad (6)$$

holds, with $j,k,l,m = 1,\ldots,N$. The effective interaction occurring among mode amplitudes reads

$$G_{jklm} = \frac{\iota}{2}\sqrt{\omega_j\omega_k\omega_l\omega_m}\int_V d^3r\,\chi^{(3)}_{\alpha\beta\gamma\delta}(\omega_j,\omega_k,\omega_l,\omega_m;\mathbf{r}) \times E^{\alpha}_j(\mathbf{r})E^{\beta}_k(\mathbf{r})E^{\gamma}_l(\mathbf{r})E^{\delta}_m(\mathbf{r}), \quad (7)$$

with $\alpha,\beta,\gamma,\delta = x,y,z$. This coefficient represents the spatial overlap of the electromagnetic fields of the modes modulated by the nonlinear susceptibility $\chi^{(3)}$. The disorder is induced, e.g., by the random spatial distribution of the scatterers (as in random lasers) that leads to randomly distributed modes and, hence, to random susceptibilities and couplings among quadruple modes.

If the cavity is open, the mode set is no more complete, the modes whose profile decays exponentially out of the cavity are taken for the expansion (4), all the others form the radiation modes. Under the standard approach,[41–45] the coefficients in the expansion that weight the radiation modes can be expressed in terms of the disordered cavity one, and this results in linear terms in the Hamiltonian (open cavity regime). Thus, for an open cavity, Eq. (5) becomes

$$\mathcal{H} = -\Re\left[\sum_{j<k} G^{(2)}_{jk}a_j a^*_k + \sum_{\omega_j+\omega_k=\omega_l+\omega_m} G^{(4)}_{jklm}a_j a_k a^*_l a^*_m\right]. \quad (8)$$

The Hamiltonian expressions, Eqs. (5) and (8), can be also obtained starting from the corresponding Langevin dynamical equations, as detailed, e.g., in Ref. 46:

$$\dot{a}_n(t) = \sum_j G^{(2)}_{jn}a_j + \sum_{\omega_j+\omega_n=\omega_k+\omega_l} G^{(4)}_{jkln}a^*_j a_k a_l + \eta_n(t) = -\frac{\partial\mathcal{H}}{\partial a^*_n} + \eta_n(t), \quad (9)$$

where $\eta_n(t)$ is a white noise, for which

$$\langle\eta_j(t)\eta_k(t')\rangle = 2T\delta_{jk}\delta(t-t'). \quad (10)$$

Here T is a "heat-bath" temperature, whose physical interpretation depends on the specific system. In the case of a random laser it represents the spontaneous emission and $k_BT \cong \hbar/\tau$, with τ being the amplifying level lifetime.[46,47]

Comparing Eq. (9) with the master equation for mode-locking lasers in ordered cavities,[31,41]

$$\dot{a}_n(t) = (g_n - \ell_n + i\,D_n)a_n + (\gamma - i\delta)\sum_{\omega_j+\omega_n=\omega_k+\omega_l} a^*_j a_k a_l + \eta_n(t), \quad (11)$$

we can understand the physical role played by the parameters of the probability distribution of the G's. Indeed, g_n is the gain coefficient of the nth mode in a round-trip through the cavity, ℓ_n the loss term, D_n the group velocity of the wave packet, γ the coefficient of the saturable absorber (responsible for passive mode-locking), and δ the coefficient of the Kerr lens effect. Neglecting the latter we can see that a system with a positive average of the G_{jklm} corresponds to the presence of a saturable absorber. In the case of peaked probability distribution for the couplings $P(G)$, i.e., weak disorder, the system will tend to display the same spectrum of many equally spaced modes typical of mode-locking lasers. In the present formalism this will be a ferromagnetic phase. One might, then, wonder what happens when the disorder is so strong as to prevent the occurrence of this phase and, even, when the random coefficient corresponding of γ is negative (i.e., when passive mode-locking is absent). We discuss this issue in Sec. II A.

In the "strong cavity limit," the linear coupling between modes is negligible, $G^{(2)}_{mn}$ is diagonal (i.e., one accounts only for the finite-lifetime of the modes), and

$$\mathcal{H} = -\Re\left[\sum_{i=1}^{N} G^{(2)}_{ii}|a_i|^2 + \sum_{\omega_{i_1}+\omega_{i_3}=\omega_{i_2}+\omega_{i_4}} G^{(4)}_{i_1i_2i_3i_4}a_{i_1}a_{i_3}a^*_{i_2}a^*_{i_4}\right]. \quad (12)$$

Note that the modes in the disordered cavity may display a different degree of localizations, as in the case of disordered PhC. Correspondingly, the distribution of the overlaps G spreads. Moreover, the constituents of the overlap integral are also very difficult to calculate from first principles. Indeed, to our knowledge, the only specific form of the nonlinear susceptibility has been computed by Lamb[48] for a two-level system (without disorder). Eventually, to estimate the coupling distribution from the experimental data is a very complicated inverse statistical problem (cf., e.g., Refs. [49,50] and references therein), and, so far, the reconstruction of the G's, for example, from measurements of random laser spectra has never been achieved. The interplay between susceptibility and spatial distribution of modes leading to G's is, then, a very challenging problem that deserves a systematic and sophisticated treatment that goes beyond the aim of the present work.

In the following we consider a mean-field approach in which all modes are connected with each other. We, thus, approach the study of our model by means of Gaussian distributed G's with nonvanishing average, as detailed below.

The leading regime considered in this work is, actually, driven by a *quenched amplitude approximation*, which is obtained by retaining the amplitudes $A_n = |a_n|$ (and correspondingly the energies of the modes) as slowly varying with respect to the phase $\phi_n = \arg(a_n)$, such that the resulting interaction Hamiltonian [retaining only those terms depending on the phases, and considering the strong or closed cavity regime, cf. Eq. (12)], turns out to be[32,46]

$$\mathcal{H} = -\sum_{\omega_{i_1}+\omega_{i_3}=\omega_{i_2}+\omega_{i_4}}{}' G_{i_1i_2i_3i_4}A_{i_1}A_{i_2}A_{i_3}A_{i_4} \times \cos(\phi_{i_1}+\phi_{i_3}-\phi_{i_2}-\phi_{i_4}), \quad (13)$$

where the sum $\sum'$ is limited to those terms that depend on the phases (i.e., we neglect terms whose indices are such that the argument of the cosine vanishes, e.g., $i_1 = i_2$ and $i_3 = i_4$) and G is assumed to be real valued.

Actually, in the physical systems of our interest, it is not necessary that the resonant condition Eq. (6) for having four modes interact in the mode-locking regime be satisfied exactly. Indeed, it is enough that the mode combination tone ω_{i_1} lies inside an interval around $\omega_{i_2}+\omega_{i_4}-\omega_{i_3}$ corresponding to its linewidth.[51] In the case, e.g., of the random laser, in which many modes oscillate in a relatively small bandwidth

and are densely packed in frequency space so that the their linewidths overlap, this observation supports the further mean-field-like approximation $\omega_i \simeq \omega_0, \forall i$. In our model, therefore, the spectral distribution of the angular frequencies will be considered as strongly peaked around ω_0 and $\omega_{i_1} + \omega_{i_3} \simeq \omega_{i_2} + \omega_{i_4} \simeq 2\omega_0$, so that the "selection rule," Eq. (6), is always satisfied.

A suitable normalization and the introduction of an inverse temperaturelike parameter β leads, eventually, from Eq. (13) to

$$\beta\mathcal{H}_J[\phi] = -\beta \sum_{\substack{i_1 < i_2, i_3 < i_4 \\ i_1 < i_3}}^{N} J_{\mathbf{i}} \cos(\phi_{i_1} + \phi_{i_2} - \phi_{i_3} - \phi_{i_4}), \tag{14}$$

with

$$\beta \equiv \frac{\langle A^2\rangle^2}{k_B T_{\text{bath}}} \tag{15}$$

$$J_{\mathbf{i}} = J_{i_1 i_2 i_3 i_4} \equiv \frac{G_{i_1 i_2 i_3 i_4}}{V^2} \frac{A_{i_1} A_{i_2} A_{i_3} A_{i_4}}{\langle A^2\rangle^2}, \tag{16}$$

where T_{bath} is the heat-bath temperature, variance of the white noise η, cf. Eq. (10) induced by spontaneous emission, and the squared volume factor guarantees thermodynamic convergence ($\beta\mathcal{H} \propto V \sim N$). The average energy per mode is $\mathcal{E}_0 = \omega_0 \langle A^2\rangle$. This is proportional to the so-called *pumping rate* $\mathcal{P}$ induced on the random laser by the pumping laser source. We define it as

$$\mathcal{P}^2 \equiv J_0 \frac{\langle A^2\rangle^2}{k_B T_{\text{bath}}} \tag{17}$$

encoding the experimental evidence that decreasing the heat-bath temperature[52] or increasing the energy of the pumping light source[53] has the same qualitative effect. The proportionality factor J_0 in Eq. (17) is a material-dependent parameter function of the angular frequency ω_0 of the peak of the average spectrum, cf. Eq. (7),

$$J_0 = V\omega_0^2 \int_V d^3r\, \chi^{(3)}(\omega_0; \boldsymbol{r}) |E(\boldsymbol{r})|^4, \tag{18}$$

in which $|E(\boldsymbol{r})|^2 = \langle E_n^2\rangle \sim 1/V$. Assuming that the nonlinear susceptibility does not scale with the number of modes, the above integral scales as $1/V$ and J_0 does not scale with the size of the system. The average of $J_{\mathbf{i}}$, instead, scales as $1/V^3$, according to the definitions Eqs. (8) and (16).

For the sake of qualitative comparison with the outcome of experiments the statistical mechanical inverse temperature β can be expressed in terms of the squared pumping rate as

$$\beta = \frac{\mathcal{P}^2}{J_0}. \tag{19}$$

B. Finite-temperature Bose-Einstein condensates

A similar situation is found in the finite-temperature Bose Einstein condensation with random potential. The zero-temperature Gross-Pitaevskii equations[54] reads as

$$\imath\hbar \frac{\partial \Phi}{\partial t} = -\frac{\hbar^2}{2m}\nabla^2\Phi + V_{\text{ext}}(\boldsymbol{r})\Phi + g|\Phi|^2\Phi, \tag{20}$$

where $V_{\text{ext}}(\boldsymbol{r})$ is an externally set disordered potential and $g = 4\pi\ell\hbar^2/m$, with ℓ being the s-wave scattering length. An analogous model holds for reduced-dimensionality cases.

The modes satisfy the time-independent linear Schrödinger equation

$$-\frac{\hbar^2}{2m}\nabla^2\Phi_n + V_{\text{ext}}(\boldsymbol{r})\Phi_n = E_n\Phi_n. \tag{21}$$

Their interaction can be treated variationally by letting

$$\Phi(\boldsymbol{r},t) = \sum_n a_n(t)\Phi_n(\mathbf{r}) \exp\left(-\imath\frac{E_n}{\hbar}t\right). \tag{22}$$

A finite-temperature model for BEC is the Stoof equation,[55,56] which is here written as

$$\imath\hbar\frac{\partial\Phi}{\partial t} = \left[1 + \hbar\frac{\beta_K}{4}\Sigma^K(\boldsymbol{r},t)\right] \times \left[-\frac{\hbar^2}{2m}\nabla^2\Phi + V_{\text{ext}}(\boldsymbol{r})\Phi + g|\Phi|^2\Phi\right] + \eta(\boldsymbol{r},t), \tag{23}$$

with $\beta_K = 1/k_B T$ (k_B is the Boltzmann constant) and where the finite-temperature noise is such that

$$\langle\eta^*(\boldsymbol{r}',t')\eta(\boldsymbol{r},t)\rangle = \frac{\imath\hbar}{2}\Sigma^K(\boldsymbol{r},t)\delta(t-t')\delta^{(3)}(\boldsymbol{r}-\boldsymbol{r}'), \tag{24}$$

with $\Sigma^K(\boldsymbol{r},t)$ being the Keldish self-energy, which is imaginary valued (for its expression see Ref. 56) and $\hbar\Sigma^K \propto -\imath\beta_K^{-2}$ (see Ref. 57). Expanding over the complete set of the zero-temperature equations, one obtains

$$\imath\hbar\dot{a}_n(t) = -\imath\sum_j \alpha_{jn}a_j E_j e^{-\frac{\imath t}{\hbar}(E_j - E_n)} + \sum_{jkl}(G_{jkln} - \imath K_{jkln})a_l^* a_j a_k e^{-\frac{\imath t}{\hbar}(E_j + E_k - E_l - E_n)} + \eta_n(t), \tag{25}$$

where $\eta_n(t) = \int d^3\mathbf{r}\eta(\mathbf{r},t)\phi_n(\mathbf{r},t)$, and the mode-overlap coefficients are defined as

$$G_{jklm} = g\int \Phi_j\Phi_k\Phi_l\Phi_m d^3\mathbf{r} \tag{26}$$

and

$$K_{jklm} = \frac{\imath\beta_K\hbar g}{4}\int \Sigma^K(\boldsymbol{r})\Phi_j\Phi_k\Phi_l\Phi_m d^3\mathbf{r}. \tag{27}$$

Finally, the linear coupling coefficients come out to be

$$\alpha_{jk} = \frac{\imath\beta_K\hbar}{4}\int \Sigma^K(\boldsymbol{r})\Phi_j\Phi_k d^3\mathbf{r}. \tag{28}$$

While retaining the synchronous terms (such that $E_j + E_k - E_l - E_n = 0$), the resulting equations are, hence, of the same form of those reported in Sec. I A for the disordered electromagnetic cavity, being the energy of the eigenstates in place of the angular frequency. Indeed, a strong coupling regime is attained when there is an enhanced region for the density of states. Conversely, in other spectral regions, both the linear and the nonlinear coupling terms are averaged out by the rapidly oscillating exponential tails.

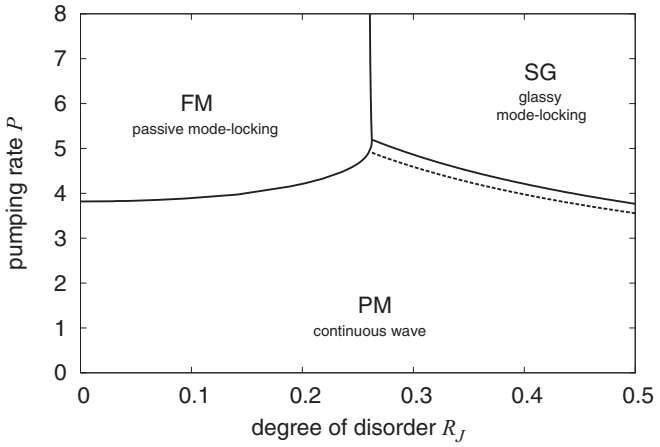

FIG. 1. Phase diagram in the $\mathcal{P}, R_J$ plane. Three phases are present: paramagnetic (PM) (low $\mathcal{P}$), ferromagnetic (FM) (high $\mathcal{P}$/weak disorder), and spin glass (SG) (high $\mathcal{P}$/strong disorder). The solid lines are thermodynamic transitions; the dashed line represents the dynamic PM/SG transition.

Let us consider, for example, a periodic external potential with some degree of disorder. In this case, a Lifshitz tail[58] is present, that is, a region with energies inside the forbidden gap corresponding to localized modes. These modes will all have approximately the same energy $E \cong E_B$, where E_B is the band-edge energy, and will couple both with each other and with the delocalized Bloch modes at the band edge. Correspondingly, the relevant equations for the strongly coupled modes are

$$\imath\hbar\dot{a}_n(t) = -\imath \sum_j \alpha_{jn} a_j E_B + \sum_{jkl} (G_{jkln} - \imath K_{jkln}) a_l^* a_j a_k + \eta_n(t). \quad (29)$$

The other modes (those far from the spectral gap) will be those mediating the thermal bath. The quenched amplitude approximation eventually leads to the phase-dependent Hamiltonian, Eq. (14).

As discussed in the following section of the manuscript, even in the zero-temperature limit a transition is expected. This corresponds to the existence of a replica symmetry breaking transition in BECs for finite and vanishing temperatures, mediated by the degree of disorder and heuristically following the phase diagram reported in Fig. 1.

We stress that for BECs in the presence of disorder it is known that a Bose-glass phase can be found in the zero-temperature limit, corresponding to a condensate fragmented into various states.[2,3,59] Here, we point out that this kind of phase may display a nonvanishing complexity depending on the degree of coherence (the relation between the phases of the modes), which is affected by the spread of the coupling coefficients (determined by the spread of the localization lengths) and by the sign and strength of the nonlinear interaction. The complete details deserve a separate paper.

C. Nonlinear optical propagation in disordered media and the zero-temperature limit

The nonlinear optical propagation of a light beam is described by the paraxial equation

$$\imath \frac{\partial A}{\partial z} + \frac{1}{2k}\nabla^2_{x,y} A + \frac{\Delta n}{2kn} A = 0, \quad (30)$$

where A is the optical amplitude, k is the wave number, n is the bulk refractive index, and Δn is its perturbation due to disorder and optical nonlinearity (Kerr effect):

$$\frac{\Delta n}{2kn} = U(x,y) + n_2 |A|^2. \quad (31)$$

The nonlinear coefficient n_2 can be either positive (focusing) or negative (defocusing), while $U(x,y)$ can be a perturbed (by disorder) periodical potential or a completely disordered (speckle pattern) external potential. The resulting equation reads

$$\imath \frac{\partial A}{\partial z} + \frac{1}{2k}\nabla^2 A + U(x,y)A + \frac{n_2}{2kn}|A|^2 A = 0. \quad (32)$$

This formally corresponds (with different meanings for the variable) to the zero-temperature two-dimensional limit of the Gross-Pitaevskii equations detailed above, cf. Eq. (20).

In this case, as well, the field can be expanded in terms of transversely localized (in two dimensions they are always localized) electromagnetic modes, the energies being replaced by their propagation wave vectors. When there are a bunch of modes such that their wave vectors are similar, these will be strongly coupled and result in dynamical equations like Eqs. (9) and (29). This approach can be extended to three-dimensional propagation, encompassing the dynamics of ultrashort pulses in random media as will be reported elsewhere.

The replica symmetry breaking transitions investigated in the following in general correspond to varying coherence properties of the beam, eventually resulting in unstable speckle patterns. The $\beta \to \infty$ limit of the statistical mechanics formulation of the problem has to be taken in this case (see, e.g., Ref. 60 for a simple case example in the framework of constraint satisfaction problems).

II. RANDOMNESS IN MODE-COUPLING COEFFICIENTS

Let us consider our model Hamiltonian, Eq. (13), in the mean-field fully connected approximation in which the nonvanishing components of the four-index tensor $J_{i_1,i_2,i_3,i_4} = J_{\mathbf{i}}$ are distributed as

$$\overline{J_{\mathbf{i}}} = J_0/N^3, \quad (33)$$

$$\overline{(J_{\mathbf{i}} - \overline{J_{\mathbf{i}}})^2} = \sigma_J^2/N^3. \quad (34)$$

The coefficient J_0 was already introduced in the case of random lasers, cf. Eq. (18), and N is the number of dynamic variables (mode phases) of the system, proportional to the volume V. The overbar denotes the average over the disorder.

To quantify the amount of disorder, we introduce the "degree of disorder" parameter, i.e., a size-independent ratio

between the standard deviation of the distribution of the coupling coefficients J_i and their mean:

$$R_J \equiv \frac{\sigma_J}{J_0} \tag{35}$$

The limits $R_J \to 0$ and $R_J \to \infty$ correspond, respectively, to the completely ordered case and the disordered case. The other relevant parameter for our investigation is the inverse temperature β. For random lasers it is related to the normalized pumping threshold for ML, defined in our model as, cf. Eq. (19),[61]

$$\mathcal{P} = \sqrt{\beta J_0} = \sqrt{\frac{\bar{\beta}}{R_J}}, \tag{36}$$

where $\bar{\beta} \equiv \beta\sigma_J$.[32] In general, β increases as the strength of nonlinearity increases or as the amount of noise is reduced.

A. The ordered limit, saturable absorbers in random lasers, defocusing versus focusing

With specific reference to the laser systems, as J_0 grows the effect of disorder is moderated and for small enough R_J the model corresponds to the ordered case, previously detailed in Ref. 62. As also previously reported in Ref. 63, a passive mode-locking (PML) transition is predicted as a paramagnetic (PM)/ferromagnetic (FM) transition occurs in β.

Indeed, in our units, when $R_J \to 0$, $\mathcal{P} = \mathcal{P}_{\rm PML} \cong 3.819$ (see Fig. 1), in agreement with the ordered case.[45,64] As explained below, the deviation from this value quantifies an increase of the standard mode-locking (ML) threshold $\mathcal{P}_{\rm PML}$ due to disorder. The specific value for $\mathcal{P}_{\rm PML}$ will depend on the class of lasers under consideration (e.g., a fiber loop laser or a random laser with paint pigments), but the trend of the passive ML threshold with the strength of disorder R_J in Fig. 1 has a universal character. The pumping rate $\mathcal{P}$ contains J_0: for a fixed disorder the threshold will depend on the nonlinear mode-coupling.

A key point here is that the transition from continuous wave to passive mode-locking (PM $\to$ FM) only occurs for a specific sign of the mean value of the coupling coefficient J_0, as shown in Fig. 2. Comparing Eqs. (9) and (11) one observes that this formally corresponds to the presence of a saturable absorber in the cavity (see also Ref. 31 and Sec. I A). In typical random lasers such a device is not present, and, hence, this ferromagnetic transition is not expected.

On the other hand, the reported phase diagram, Fig. 2, predicts that starting from a standard laser supporting passive mode-locking and increasing the disorder the second-order transition acquires the character of a glass transition. A notable issue is that this phase-locking transition (normally ruled out for ordered lasers without a saturable transition) spontaneously occurs increasing β, as an effect of the disorder and the resulting frustration.

With reference to nonlinear waves, the spontaneous phase-locking process is expected for a specific sign of the nonlinear susceptibility (corresponding to repulsive interactions for BEC and defocusing nonlinearities for optical spatial beams), for $T = 0$, amounting to $J_0/\sigma_J > 0$ in Fig. 2 (the threshold is at $J_0/\sigma_J \cong 4$). For example, for a nonlinear optical beam propagating in a disordered medium, it is expected that above a certain degree of disorder there is a transition from a coherent regime to a "glassy coherent phase," characterized by a strong variation from shot to shot of the speckle pattern and, more in general, of the degree of spatial coherence.

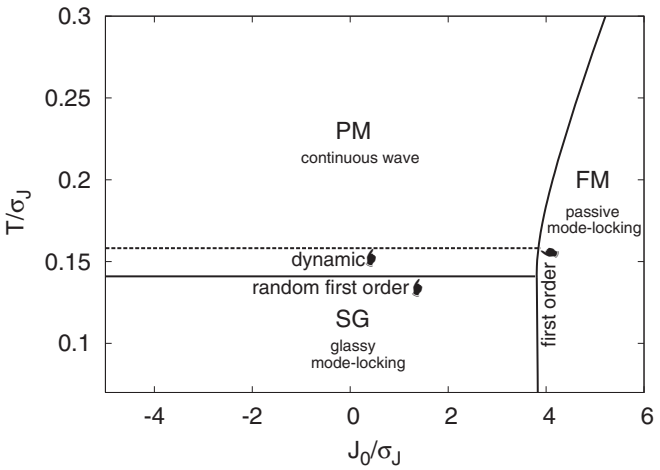

FIG. 2. Phase diagram in the plane J_0, T in σ_J units. Also negative J_0 are considered. Three phases are found: PM (high T, low J_0), FM (low T/large J_0). and SG (low T/low or negative J_0). The solid lines are thermodynamic transitions: *random* first order between PM and SG and *standard* first order between PM and FM and between SG and FM. The dashed line represents the dynamic PM/SG transition.

III. FUNDAMENTALS OF STATISTICAL MECHANICS OF DISORDERED SYSTEMS

Hereby we report an extremely concise summary of ideas and techniques developed to deal with disordered systems. The aim is to let the nonexpert reader find his/her way through the computation of the properties of our model that we present in Sec. IV and the Appendix.

A. Disorder and frustration: Quenched disorder as technical tool

The main issue determining complex features, not present in ordered systems and involving collective processes that cannot be understood just looking at local properties, is *frustration*. This is usually the consequence of disorder, not necessarily *quenched* disorder though. Indeed, also in materials whose effective statistical mechanical representation is carried out through deterministic potentials (as, e.g., for colloidal particles), a geometry-induced disorder can occur, determining frustration and a consequent multitude of degenerate stable and metastable states typical of glasses[65–72] and spin glasses.[73–75] Quenched disorder, i.e., the explicit appearance of random coefficients in the Hamiltonian, allows an analytic computation, but the results are general and do not depend on the specific source of frustration.

B. Statistical mechanics of a disordered system: The replica trick

In the presence of quenched disorder, one can compute the statistical mechanics of the system, averaging over the probability distribution of the disorder. In order to do this the

so-called replica trick[76–79] can be adopted or else the equivalent cavity method.[79,80]

The free energy of a single disordered system sample, denoted by J, is $\Phi_J = -(1/\beta)\log Z_J$. Correspondingly, the physically relevant average free energy can be written as

$$\Phi = -\frac{1}{\beta}\overline{\log Z_J}, \tag{37}$$

where the overbar denotes the average over the distribution of the J's. The latter coincides with the thermodynamic limit of any Φ_J according to the self-averaging property required in order to have macroscopic reproducibility of experiments (the thermodynamics of a huge system does not depend on the local distribution of interaction couplings).

To perform the average in Eq. (37) is highly nontrivial and one can proceed by considering n copies of the system, Eq. (13),

$$\mathcal{H}[\{\phi\}] \to \sum_{a=1}^{n}\mathcal{H}[\{\phi^{(a)}\}]. \tag{38}$$

The average free energy per spin can then be computed in the replicated system as

$$\beta\Phi = -\lim_{N\to\infty}\frac{1}{N}\overline{\log Z_J} = -\lim_{N\to\infty}\lim_{n\to 0}\frac{\overline{Z_J^n}-1}{Nn}, \tag{39}$$

where the average of the generic power of the partition function $\overline{Z_J^n}$ is somehow computed for a finite integer n and, eventually, the analytic continuation to real n and the limit $n \to 0$ is performed.

C. Oddities of the replica formulation

Actually, to evaluate $\overline{Z_J^n}$, one makes use of the saddle-point approximation holding for large N (see the Appendix for the specific case considered in this work). That is, one practically inverts the limits $N \to \infty$ and $n \to 0$ as expressed in Eq. (39). Yet, the method works. It took many years to rigorously overcome this oddity and a mathematical proof of the existence of the free energy can be found in Refs. 81 and 82.

D. A probability distribution as an order parameter

The main novelty of the characterization of the spin-glass phase, historically first obtained by the replica method and subsequently confirmed by other methods, is that the order parameter is a whole probability distribution function describing how different thermodynamic states are correlated. The degree of the correlation between two states is called *overlap*. In mean-field theory different states exist that can be more or less correlated according to their distance on a treelike hierarchical space called *ultrametric*.[83]

E. Complexity as a well-defined thermodynamic potential

Besides numerous and hierarchically organized globally stable states, glasses also display a large number of metastable states, that is, excited states with relatively long lifetimes. In the mean-field theory such a lifetime is, actually, infinite in the thermodynamic limit because of the divergence of the free energy barriers with the size of the system, see, e.g., Ref. 84. This means that, contrary to what happens in real glasses,[85] the number of metastable states at a given observation time scale does not change with time (after a given transient period). Below a certain temperature (called *dynamic* or *mode coupling* temperature), the number $\mathcal{N}$ of metastable states grows exponentially with the size N of the system (N being the number of modes in our case). One can then define an entropylike function counting the metastable states as

$$\Sigma \equiv \frac{1}{N}\log\mathcal{N}. \tag{40}$$

This is called *configurational entropy* in the framework of structural glasses, or *complexity* in spin-glass theory and its applications to constraint satisfaction and optimization problems. One can further look at the metastable states of equal free energy density f: $\mathcal{N}(f) = \exp N\Sigma(f)$ and at the free energy interval, above the equilibrium free energy $f_{\rm eq}$, in which the complexity is nonzero: $f \in [f_{\rm eq} : f_\star]$.

IV. STATISTICAL MECHANICAL PROPERTIES

Starting from the Hamiltonian, Eq. (13), replicated according to the prescription Eq. (38), and averaging over the disorder with the Gaussian probability expressed by Eqs. (33) and (34), one obtains the following expression for the average of the nth power of the partition function (cf. the Appendix):

$$\overline{Z_J^n} = \int \mathcal{D}\mathbf{Q}\mathcal{D}\Lambda e^{-NnG[\mathbf{Q},\Lambda]}, \tag{41}$$

$$\begin{aligned} nG[\mathbf{Q},\Lambda] &= nA[\mathbf{Q},\Lambda] - \log Z_\phi[\Lambda], \\ nA[\mathbf{Q},\Lambda] &\equiv -\frac{\beta^2\sigma_J^2}{32}\sum_{a=1}^{n}(1+|\tilde r_a|^4) \\ &\quad -\frac{\beta J_0}{8}\sum_{a=1}^{n}|\tilde m_a|^4 - \frac{\beta^2\sigma_J^2}{16}\sum_{a<b}^{1,n}\left(q_{ab}^4+|r_{ab}|^4\right) \\ &\quad +\sum_{a<b}^{1,n}[q_{ab}\lambda_{ab}+\Re(r_{ab}\bar\mu_{ab})] \\ &\quad +\sum_{a=1}^{n}\Re[\tilde r_a\bar{\tilde\mu}_a+\tilde m_a\bar\nu_a], \end{aligned} \tag{42}$$

$$Z_\phi[\Lambda] \equiv \int\prod_{a=1}^{n}d\phi_a e^{-\beta\mathcal{H}_{\rm eff}[\{\phi\};\Lambda]} \tag{43}$$

$$\begin{aligned} -\beta\mathcal{H}_{\rm eff}[\{\phi\};\Lambda] &\equiv \sum_{a<b}^{1,n}\Re[e^{\imath(\phi_a-\phi_b)}\lambda_{ab}+e^{\imath(\phi_a+\phi_b)}\bar\mu_{ab}] \\ &\quad +\sum_{a=1}^{n}\Re[e^{2\imath\phi_a}\bar{\tilde\mu}_a+e^{\imath\phi_a}\bar\nu_a], \\ \mathcal{D}\mathbf{Q} &\equiv \prod_{a<b}^{1,n}N^4dq_{ab}dr_{ab}\times\prod_{a=1}^{n}N^4d\tilde r_a d\tilde m_a \\ \mathcal{D}\Lambda &\equiv \prod_{a<b}^{1,n}\frac{d\lambda_{ab}}{2\pi}\frac{d\mu_{ab}}{2\pi}\times\prod_{a=1}^{n}\frac{d\tilde\mu_a}{2\pi}\frac{d\nu_a}{2\pi}, \end{aligned} \tag{44}$$

with $dy_{ab} = dy^R_{ab} dy^I_{ab}$. where $\mathbf{Q} = \{q,r,\tilde{r},\tilde{m}\}$ and $\Lambda = \{\lambda,\mu,\tilde{\mu},\nu\}$. The overlap matrices q_{ab} and λ_{ab} are real valued, whereas the others have complex elements.

The integral Eq. (41) is evaluated by means of the saddle-point approximation (valid for large N). The above expressions need a form of the matrices q_{ab}, r_{ab}, λ_{ab}, and μ_{ab} to be completed. Contrary to what might seem reasonable, the form providing the thermodynamically stable solution is not the one in which all replicas are equivalent, i.e., all elements in the matrices q_{ab}, r_{ab}, λ_{ab}, and μ_{ab} are equal. One must, thus, resort to a spontaneous *replica symmetry breaking*. In the Appendix we report the computation of thermodynamics both in the replica symmetric (RS) approximation and in the "one step" replica symmetry breaking ansatz (1RSB), i.e., the exact solution for the system under probe. In the following we, thus, analyze the properties of the latter solution.

Spin-glass systems described by more-than-two-body interactions, cf. Eq. (13), are known to have low-temperature phases that are stable under the 1RSB ansatz.[86–88] Under this ansatz, taking the $n \to 0$ limit, the free energy functional $\beta\Phi$ reads (cf. the Appendix),

$$\begin{aligned}
&\beta\Phi\big(m;\mathbf{Q}^{(1)}_{\rm sp},\Lambda^{(1)}_{\rm sp}\big)\\
&\quad= G\big(m;\mathbf{Q}^{(1)}_{\rm sp},\Lambda^{(1)}_{\rm sp}\big)\\
&\quad= -\frac{\bar\beta R_J}{8}|\tilde m|^4 - \frac{\bar\beta^2}{32}\big[1-(1-m)\big(q_1^4+|r_1|^4\big)\\
&\qquad - m(q_0^4+|r_0|^4) + |r_d|^2\big] - \Re\bigg[\frac{1-m}{2}(\lambda_1 q_1 + \bar\mu_1 r_1)\\
&\qquad + \frac{m}{2}(\lambda_0 q_0 + \bar\mu_0 r_0) - \bar\mu_d r_d - \bar\nu\tilde m\bigg] + \frac{\lambda_1}{2}\\
&\qquad - \frac{1}{m}\int \mathcal{D}[\mathbf{0}]\log\int\mathcal{D}[\mathbf{1}]\bigg[\int_0^{2\pi} d\phi\,\exp\mathcal{L}(\phi;\mathbf{0},\mathbf{1})\bigg]^m,
\end{aligned} \tag{45}$$

where $\mathbf{0} = \{x_0,\zeta_0^R,\zeta_0^I\}$, $\mathbf{1} = \{x_1,\zeta_1^R,\zeta_1^I\}$, $\mathcal{D}[\boldsymbol{a}]$ is the product of three normal distributions, and

$$\begin{aligned}
\mathcal{L}(\phi;\mathbf{0},\mathbf{1}) \equiv \Re\Big\{ e^{\imath\phi}\big[\bar\zeta_1\sqrt{\Delta\lambda - |\Delta\mu|} + \bar\zeta_0\sqrt{\lambda_0 - |\mu_0|}\\
+ x_1\sqrt{2\Delta\bar\mu} + x_0\sqrt{2\bar\mu_0} + \bar\nu\big] + e^{2\imath\phi}\Big(\bar\mu_d - \frac{\bar\mu_1}{2}\Big)\Big\},
\end{aligned} \tag{46}$$

with $\Delta\lambda = \lambda_1 - \lambda_0$ and $\Delta\mu = \mu_1 - \mu_0$. For later convenience we define the following averages over the action $e^{\mathcal{L}}$ [cf. Eq. (46)]:

$$c_{\mathcal{L}} \equiv \langle\cos\phi\rangle_{\mathcal{L}} \equiv \frac{\int_0^{2\pi} d\phi\cos\phi e^{\mathcal{L}}}{\int_0^{2\pi} d\phi e^{\mathcal{L}}}, \tag{47}$$

$$s_{\mathcal{L}} \equiv \langle\sin\phi\rangle_{\mathcal{L}} \equiv \frac{\int_0^{2\pi} d\phi\sin\phi e^{\mathcal{L}}}{\int_0^{2\pi} d\phi e^{\mathcal{L}}}. \tag{48}$$

The values of the order parameters $\lambda_{0,1},\mu_{0,1},\mu_d$, and ν are yielded by

$$\lambda_{0,1} = \frac{\bar\beta^2}{4}(q_{0,1})^3; \quad \mu_{0,1} = \frac{\bar\beta^2}{4}|r_{0,1}|^2 r_{0,1}; \tag{49}$$

$$\tilde\mu = \frac{\bar\beta^2}{8}|\tilde r|^2\tilde r; \quad \nu = \frac{\bar\beta R_J}{2}|\tilde m|^2\tilde m. \tag{50}$$

The parameter m (without a tilde), whose meaning is discussed below, takes values in the interval $[0,1]$. The remaining parameters are obtained by solving the following self-consistency equations:

$$q_1 = \big\langle\big\langle c^2_{\mathcal{L}}\big\rangle_m\big\rangle_{\mathbf{0}} + \big\langle\big\langle s^2_{\mathcal{L}}\big\rangle_m\big\rangle_{\mathbf{0}}, \tag{51}$$

$$q_0 = \big\langle\langle c_{\mathcal{L}}\rangle^2_m\big\rangle_{\mathbf{0}} + \big\langle\langle s_{\mathcal{L}}\rangle^2_m\big\rangle_{\mathbf{0}}, \tag{52}$$

$$r_1 = \big\langle\big\langle c^2_{\mathcal{L}}\big\rangle_m\big\rangle_{\mathbf{0}} - \big\langle\big\langle s^2_{\mathcal{L}}\big\rangle_m\big\rangle_{\mathbf{0}} + 2\imath\,\langle\langle c_{\mathcal{L}}s_{\mathcal{L}}\rangle_m\rangle_{\mathbf{0}}, \tag{53}$$

$$r_0 = \big\langle\langle c_{\mathcal{L}}\rangle^2_m\big\rangle_{\mathbf{0}} - \big\langle\langle s_{\mathcal{L}}\rangle^2_m\big\rangle_{\mathbf{0}} + 2\imath\,\langle\langle c_{\mathcal{L}}\rangle_m\rangle_{\mathbf{0}}\langle\langle s_{\mathcal{L}}\rangle_m\rangle_{\mathbf{0}}, \tag{54}$$

$$\tilde r = \langle\langle e^{2\imath\phi}\rangle_{\mathcal{L}}\rangle_m\rangle_{\mathbf{0}}, \qquad \tilde m = \langle\langle e^{\imath\phi}\rangle_{\mathcal{L}}\rangle_m\rangle_{\mathbf{0}}, \tag{55}$$

where the averages are defined as

$$\langle(\cdots)\rangle_m \equiv \frac{\int\mathcal{D}[\mathbf{1}](\cdots)\big[\int_0^{2\pi} d\phi e^{\mathcal{L}(\phi;\mathbf{0},\mathbf{1})}\big]^m}{\int\mathcal{D}[\mathbf{1}]\big[\int_0^{2\pi} d\phi e^{\mathcal{L}(\phi;\mathbf{0},\mathbf{1})}\big]^m}, \tag{56}$$

$$\langle(\cdots)\rangle_{\mathbf{0}} \equiv \int\mathcal{D}[\mathbf{0}](\cdots). \tag{57}$$

These equation are solved numerically by an iterative method. The overlap parameters $q_{0,1}$ are real valued, whereas $r_{0,1},\tilde r$, and $\tilde m$ are complex. "One-step" parameters $X_{0,1}$ ($X = q,r$) enter with a probability distribution that can be parametrized by the so-called *replica symmetry breaking parameter* m, such that

$$P(X) = m\delta(X - X_0) + (1-m)\delta(X - X_1). \tag{58}$$

The resulting independent parameters (there are ten of them) that can be evaluated by solving Eqs. (51)–(55) must be combined with a further equation for the parameter m. This is strictly linked to the expression for the *complexity* function of the system.

V. COMPLEXITY

In the order parameter Eqs. (49)–(55) m is left undetermined. An additional condition is needed to fix the value for this parameter. The first possibility is treating m as a standard order parameter: in this case the thermodynamic state corresponds to extremizing the replicated free energy (thus *maximizing* it),[89] i.e., implementing the self-consistency equation

$$\frac{\partial\Phi(m;\mathbf{Q}_{\rm sp},\mathbf{\Lambda}_{\rm sp})}{\partial m} = 0. \tag{59}$$

The highest temperature at which a solution exists with $m \leqslant 1$ furnishes a transition temperature between paramagnet and glassy phases: the Kauzmann or *static* temperature (T_s). This is an *equilibrium thermodynamic* phase transition.

This approach, however, does not reflect the known physical circumstance in which a glassy system exhibits excited metastable states also at temperature T above T_s,[90] where the equilibrium phase is paramagnetic. Vitrification, indeed, is due to the presence of a nonvanishing complexity at a temperature above T_s (and below some $T_d > T_s$), i.e., to the presence of a number of energetically equivalent states with free energy $f > f_{\rm eq}(T)$. Since, however, energy barriers tend to infinity in the thermodynamic limit in the mean-field approximation, the system dynamics is forever trapped in one of these states for

$T < T_d$. The temperature T_d is, thus, called *dynamic* transition temperature.

Across this transition the complexity Σ, defined in Eq. (40), starts being different from zero. Exactly at $T = T_d$ the complexity as a function of free energy, $\Sigma(f)$, has a δ-shaped nonzero peak at the free energy f_1 which corresponds to a maximum of $\Sigma(m)$ for a value of $m = m(f_1) = 1$. In our 1RSB formalism:

$$\frac{\partial \Sigma(m; \mathbf{Q}_{\rm sp}, \mathbf{\Lambda}_{\rm sp})}{\partial m} = 0 \tag{60}$$

As T decreases ($T_s < T < T_d$), the complexity is nonvanishing for an increasing range of free energies $f^* > f > f_1$ that corresponds to a range for m: $m^* < m < 1$. The complexity shows a maximum for $m \leqslant 1$ at the m_* ($f = f_*$) solution of $d\Sigma/dm = 0$, while it is at its minimum value for $m = 1$ and $f = f_1$. We stress that this is not a solution to Eq. (59).

Lowering the temperature, at $T = T_s$ the minimum value of complexity—corresponding to $m = 1$—vanishes, i.e., it is a solution to Eq. (59), and $f_1 = f_{\rm eq}$ corresponds to the free energy density of the global glassy minima of the free energy landscape. As mentioned above, we are in the presence of a thermodynamic phase transition and the thermodynamic stable phase is a glass.

The physically significant value for m is m^*, corresponding to the maximum of Σ. It denotes the value of free energy f^* where the number of states is maximum and exponentially higher than the number of states at any $f < f^*$ and, hence, the most probable (among those of the metastable states). At the thermodynamic transition point from the paramagnetic state to the glassy ($T = T_s$) state, it holds that $f_{\rm PM} = f_1 = f_{\rm eq} = \Phi$.[91] Below T_s $f_1 < f_{\rm eq}$ [hence, $\Sigma(f_*) < \Sigma(f_{\rm eq}) = 0$] and the physically relevant $\Sigma(f)$ has a support $[f_{\rm eq}, f_*]$.

In the following we analyze the whole complexity vs free energy curve $\Sigma(f)$ at given β and J_0 and the behavior of the minimal positive complexity $\Sigma(T)$ [and $\Sigma(\mathcal{P})$] between T_s and T_d.

A. Computing the complexity functional

In Eq. (40) one needs to know the number of metastable states, which are the local minima of the free energy landscape. Had we known the landscape, though, we would have solved the problem already. If self-consistency equations for local order parameters are known, a possible analytic approach to get information on the complex landscape is to guess a trial free energy functional whose stationary equations lead back to the self-consistency equations. This is what Thouless, Anderson, and Palmer (TAP) proposed in the framework of spin glasses starting from the self-consistency equations for local magnetizations.[92] Starting from the TAP functional and TAP equations and considering solutions to the TAP equations as *states* (with some assumptions to be *a posteriori* satisfied) one can build the functional Σ from Eq. (40), cf., e.g., Refs. [93–100].

A comparative study of the TAP-derived complexity functional and the replicated free energy, computed in a general scheme that includes the Parisi ansatz,[101] allows one to show that the Legendre transform of Φ with respect to the single-state free energy coincides with Eq. (40). According to this approach, in our model the complexity can, thus, be explicitly computed as the Legendre transform of Eq. (45):

$$\begin{aligned}
&\Sigma(m; \mathbf{Q}_{\rm sp}, \mathbf{\Lambda}_{\rm sp}) \\
&\quad = \min_m [-\beta m \Phi(m) + \beta m f] \\
&\quad = \beta m^2 \frac{\partial \Phi}{\partial m} \\
&\quad = \frac{3}{4}\beta^2 m^2 (|q_1|^4 + |r_1|^4 - |q_0|^4 - |r_0|^4) \\
&\qquad + \int \mathcal{D}[\mathbf{0}] \log \int \mathcal{D}[\mathbf{1}] \left[\int_0^{2\pi} d\phi \exp \mathcal{L}(\phi; \mathbf{0}, \mathbf{1}) \right]^m \\
&\qquad - m \int \mathcal{D}[\mathbf{0}] \left\langle \log \int_0^{2\pi} d\phi \exp \mathcal{L}(\phi; \mathbf{0}, \mathbf{1}) \right\rangle_m ,
\end{aligned} \tag{61}$$

where the single-state free energy

$$f = \frac{\partial (m\Phi)}{\partial m} \tag{62}$$

is conjugated to m. Since the above expression is proportional to $\partial \Phi / \partial m$, equating $\Sigma = 0$ provides the missing equation to determine the order parameter values.

VI. PHASE DIAGRAM AND COMPLEXITY

By varying the normalized pumping rate $\mathcal{P}$ and the degree of disorder R_J, we find three different phases, as shown in Fig. 1 in the $(\mathcal{P}, R_J)$ plane and in Figs. 2 and 3 in the (T, J_0) plane.

Paramagnetic phase. For low $\mathcal{P}$ the only phase present is completely disordered: all order parameters are zero and we have a "paramagnet" (PM); for the random laser case this phase is expected to correspond to a noisy continuous wave emission, and all the mode-phases are uncorrelated. Actually, this phase

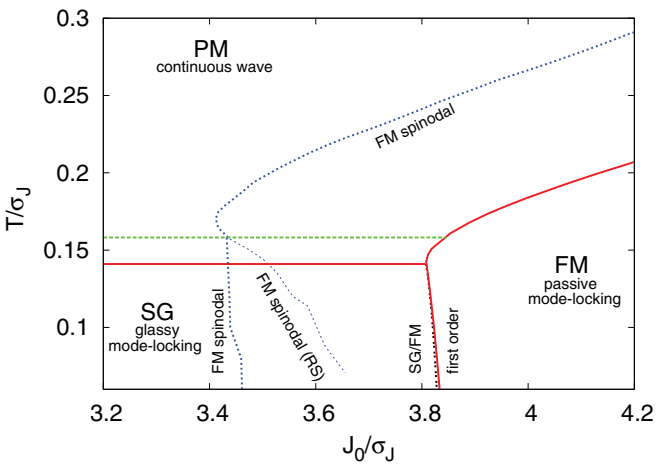

FIG. 3. (Color online) Detail of the J_0, T phase diagram around the tricritical point. Solid lines are thermodynamic transitions. Also the transition between the SG (1RSB) and the approximated RS solution for the FM phase is displayed (double-dotted line) showing no appreciable difference with the exact one. The dashed line represents the dynamic PM/SG transition. The dotted bold line represents the FM spinodal lines inside both the PM and the SG phases. The spinodal of the RS FM phase is shown as well (smaller dots).

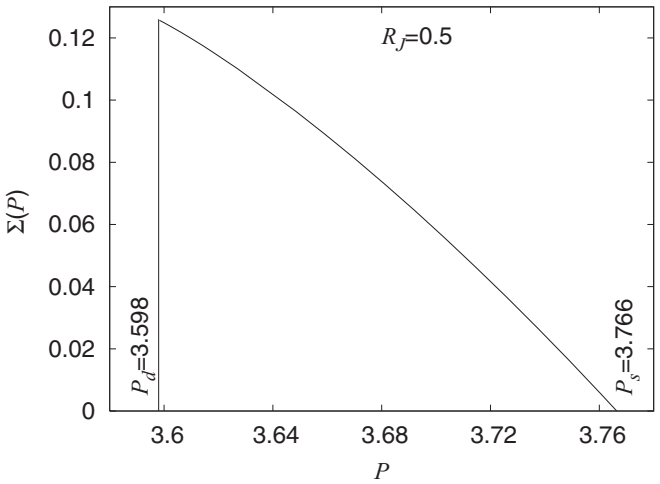

FIG. 4. Complexity $\Sigma(\mathcal{P})$ of the lowest lying glassy states in free energy between the values of the pumping rate corresponding to the dynamic and static transitions from the PM to the SG phase at $R_J = 0.5$.

exists for any degree of disorder and pumping, yet it becomes thermodynamically sub-dominant as $\mathcal{P}$ (or β) increases and, depending on the degree of disorder, the spin-glass or the ferromagnetic phases take over.

Glassy phase. For large disorder, as $\mathcal{P}/\beta$ grows, a discontinuous transition occurs from the PM to a spin-glass (SG) phase in which the phases ϕ are frozen but do not display any ordered pattern in space. First, along the line $\mathcal{P}_d = \sqrt{\bar{\beta}_d/R_J}$, in Fig. 1, or at $T/\sigma_J = 1/\bar{\beta}_d = 0.154\,47$, in Figs. 2 and 3 (dashed lines), a dynamic transition occurs. Indeed, the lifetime of metastable states is infinite in the mean-field model and the dynamics gets stuck in the highest lying excited states. The thermodynamic state is, however, still PM. Figure 3 displays a detail of the tricritical region where, besides thermodynamic transition lines, we also plot as dotted curves the lines at which the ferromagnetic phase first appears as metastable, i.e., the spinodal lines.

In Fig. 4 we plot the complexity of the metastable glassy states of the lowest free energy between the dynamic and the static transition. In the left panel of Fig. 5, $\Sigma(\mathcal{P})$ is displayed

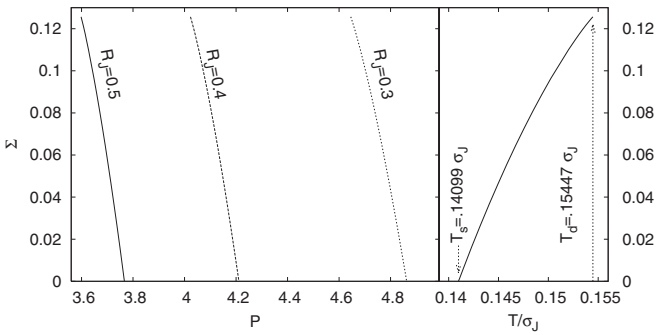

FIG. 5. Left panel: Complexity of the lowest lying glassy states in free energy $\Sigma(\mathcal{P})$ between dynamic and static transition from the PM phase to the SG phase along the $R_J = 0.3$, 0.4, and 0.5 lines. The qualitative behavior is identical for any $R_J \gtrsim 0.3$. Right panel: Σ vs the effective temperature T in σ_J units.

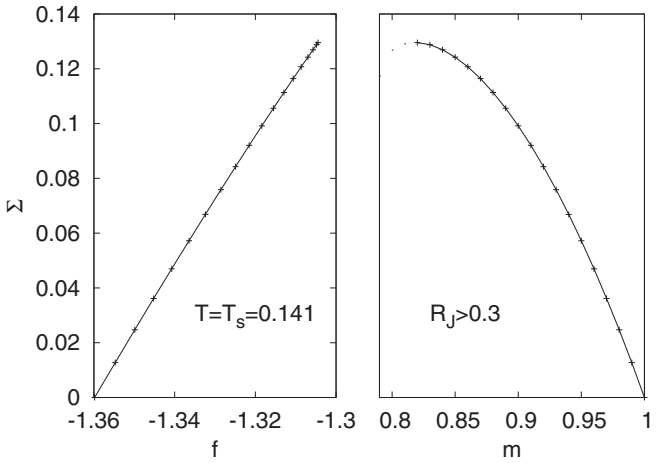

FIG. 6. $\Sigma(f)$ (left panel) and $\Sigma(m)$ (right panel) in the glassy phase at the static transition effective temperature, $T = 0.140\,99$. This is the picture that holds for any $R_J \gtrsim 0.3$.

for three different values of R_J; the threshold pumping for nonzero minimal complexity grows as the degree of disorder R_J decreases, as well as the corresponding $\mathcal{P}$ range. In the right panel $\Sigma(T)$ is plotted and it is independent of R_J. In Figs. 6 and 7 we display two instances of the whole complexity curve both vs f and m at $T = T_s$ and at a higher temperature $T < T_d$.

Across the solid line $\mathcal{P}_s(R_J) = \sqrt{\bar{\beta}_s/R_J}$, in Fig. 1 or, alternatively, across $T/\sigma_J = 1/\bar{\beta}_s = 0.140\,99$ in Fig. 2, a true thermodynamic phase transition from the continuous wave (paramagnetic) phase to the "glassy coherent light" (spin-glass) phase occurs. The order parameter q_1 [the Edwards-Anderson parameter $q_{\rm EA}$ (Ref. 102)] discontinuously jumps at the transition from zero $q_1 > q_0 = 0$, while $\tilde{m} = r_0 = r_1 = r_d = 0$ (see Fig. 8, bottom right panel). The SG phase exists for any value of R_J and $\bar{\beta} > \bar{\beta}_s$.

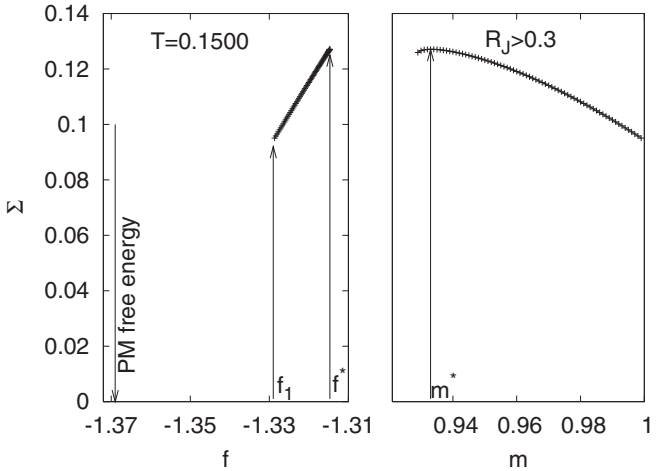

FIG. 7. $\Sigma(f)$ (left panel) and $\Sigma(m)$ (right panel) in the glassy phase at the static transition effective temperature, $T = 0.15 < T_d$. The lowest state free energy of metastable glassy states is denoted by f_1 (i.e., corresponding to $m = 1$ in the right panel, see text). The free energy of maximum complexity is denoted by f^* (correspondingly m^* in the right-hand plot).

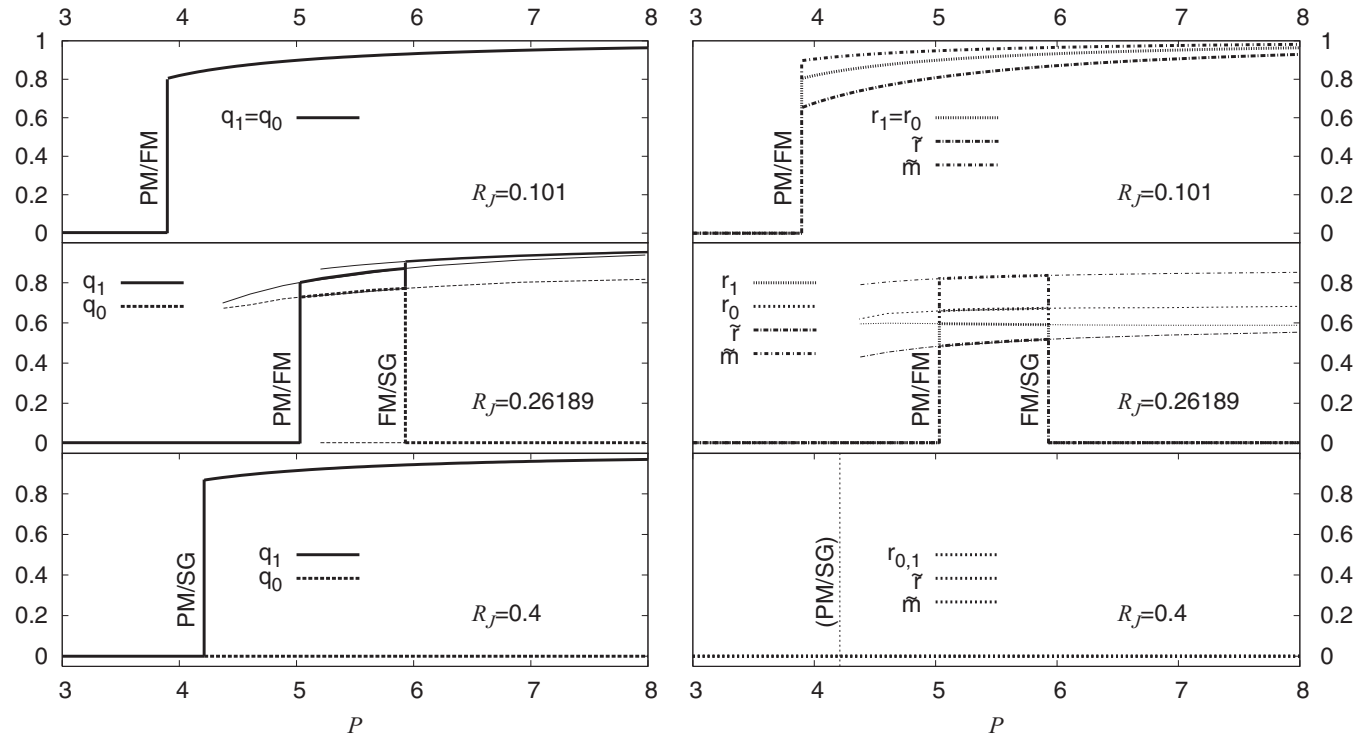

FIG. 8. Discontinuity of the order parameters at the transition points for three values of R_J. Top left panel: Jump in $q_{0,1}$, at the PM/FM transition in $\mathcal{P}$ for small disorder, $R_J \simeq 0.1$. Top right panel: Discontinuities in $r_{0,1}$, $\tilde{r}$, and $\tilde{m}$ at the same transition. For such small R_J the replica symmetry breaking is practically invisible: $q_1 \simeq q_0$, $r_1 \simeq r_0$ [to the precision of our computation, $\mathcal{O}(10^{-5})$]. Middle left panel (across tricritical region in Fig. 1: $q_{0,1}$ vs $\mathcal{P}$ at $R_J \simeq 0.26$ where, increasing the pumping rate, first a PM/FM transition occurs followed by a FM/SG one. Middle right panel: $r_{0,1}$, $\tilde{r}$, and $\tilde{m}$ vs $\mathcal{P}$ for the same interval. First-order transition points are signaled by vertical lines. Left bottom panel: $q_{0,1}$ vs $\mathcal{P}$ for large disorder, $R_J = 0.4$ across the PM/SG random first-order transition. Right bottom panel: $r_{0,1}$, $\tilde{r}$, and $\tilde{m}$ are always zero in the SG phase and in the PM phase.

In the stable SG phase, metastable states (with infinite lifetime) continue to exist so that the thermodynamic state is actually unreachable along a standard dynamics starting from a random initial condition. In Fig. 9 we plot the typical behavior of the complexity versus the single-state free energy at $T/\sigma_J = 0.1$, qualitatively identical to the left panel of Fig. 6 displaying $\Sigma(f)$ at $T = T_s$.

Ferromagnetic phase. For weak disorder a random FM phase turns out to dominate over both the SG and the PM phases. The transition PM/FM line is the standard passive ML threshold (see, e.g., Refs. [63,103]) and it turns out to be first order in the Ehrenfest (i.e., thermodynamic) sense.[85,104] From Fig. 1 we see that it takes place at growing pumping rates $\mathcal{P}$ for increasing R_J until it reaches the tricritical point with the SG phase. In the (T, J_0) plane it occurs at large—positive—J_0, cf. Fig. 2.

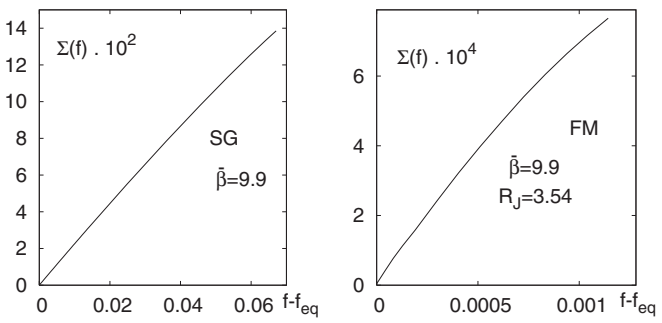

FIG. 9. Complexity vs free energy curve is plotted in the SG phase (left) at $T/\sigma_J = 0.1$ and in the FM phase (right).

To precisely describe the FM phase in the 1RSB ansatz we have to solve 11 coupled integral equations [Eqs. (51)–(55) and (59) ($\Sigma(m; \boldsymbol{Q}_{\rm sp}), \boldsymbol{\Lambda}_{\rm sp}) = 0$), cf. Eq. (61)]. In evaluating their solutions we have to consider that, in the region where the FM phase is thermodynamically dominant, both the PM and the SG solutions also satisfy the same set of equations. Besides, unfortunately, the basin of attraction of the latter two phases—in terms of initial conditions—is much broader than the FM one. Starting the iterative resolution from random initial conditions, determining the FM transition and spinodal lines becomes, thus, numerically demanding.

An approximation can be obtained by considering the RS solution for the FM phase ($\rm FM_{rs}$). This reduces the number of independent parameters to seven ($q_1 = q_0$, $r_1^{R,I} = r_0^{R,I}$, $r_d^{R,I}$, and $\tilde{m}^{R,I}$). The corresponding transition line is shown as a dashed-dotted line in Fig. 3, where, *around the transition*, we observe no practical difference with the exact SG/FM, even though the replica symmetry is clearly broken.

In Fig. 8 we show the discontinuous behavior of the order parameters across various transitions. As disorder is small (top panel) one can observe that the RSB of the solution

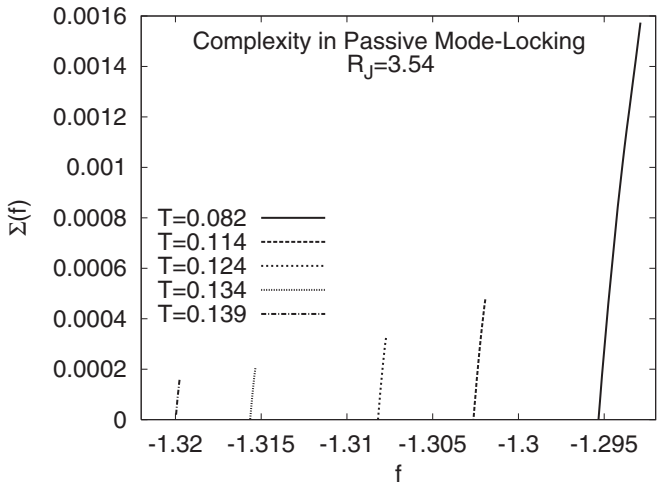

FIG. 10. Complexity curves of the FM phase at $R_J = 3.54$ at temperatures between $T = 0.082\,\sigma_J$ (right most) and $T = 0.139\,\sigma_J$ (left most). Both the magnitude of the maximal complexity and the free energy interval in which $\Sigma(f) > 0$ decreases. Notice that the equilibrium free energy decreases as the temperature increases.

representing the passive mode-locking phase vanishes, at least for what concerns the limit of precision of our computation. As the degree of disorder takes values around the tricritical point the RSB is clearly visible (middle panel), both in the FM phase and in the SG phase. For increasing disorder the FM is absent ($R_J \gtrsim 0.263$) and at high pumping/low temperature only the glassy random laser phase remains.

We must necessarily implement the 1RSB ansatz, though, to determine the nonvanishing extensive complexity, which signals the presence of a large quantity of excited states with respect to ground states, and study its behavior in T and R_J.

This, as anticipated, also implies the occurrence of a dynamic transition besides the thermodynamic one. In the phase diagrams, Figs. 1, 2, and 3, this takes place between PM and SG, where the state structure always displays a nontrivial Σ, for any $\bar{\beta} > \bar{\beta}_d$. Whether an exclusively dynamic transition can occur as a precursor to the FM phase, as well, could not be directly established in the present work. Indeed, the region of expected dynamic transition lies beyond the spinodal FM line, already very difficult to obtain numerically because of the competition with the SG and PM solutions. However, the existence of a metastable FM phase (cf. spinodal line in Fig. 3) with an extensive complexity (cf. e.g., Figs. 9 and 10) might well correspond to an arrest of the dynamic relaxation toward equilibrium of the system.

In the right-hand panel of Fig. 9 we show, e.g., $\Sigma(f)$ in the FM phase at $(R_J, \mathcal{P}) = (0.28, 5.92)$. This has to be compared with the SG complexity at the same temperature (left-hand panel of Fig. 9) that is sensitively larger and does not depend on the R_J: the maximum complexity drops about 2 orders of magnitude at the SG/FM transition, thus unveiling a corresponding *high to low complexity transition*.

In Fig. 11, at a relatively low temperature, $T = 0.0785$, we show the behavior of the 1RSB (equilibrium) free energy and order parameters across this SG (high complexity)/FM (low complexity) transition. The transition is first order in R_J.

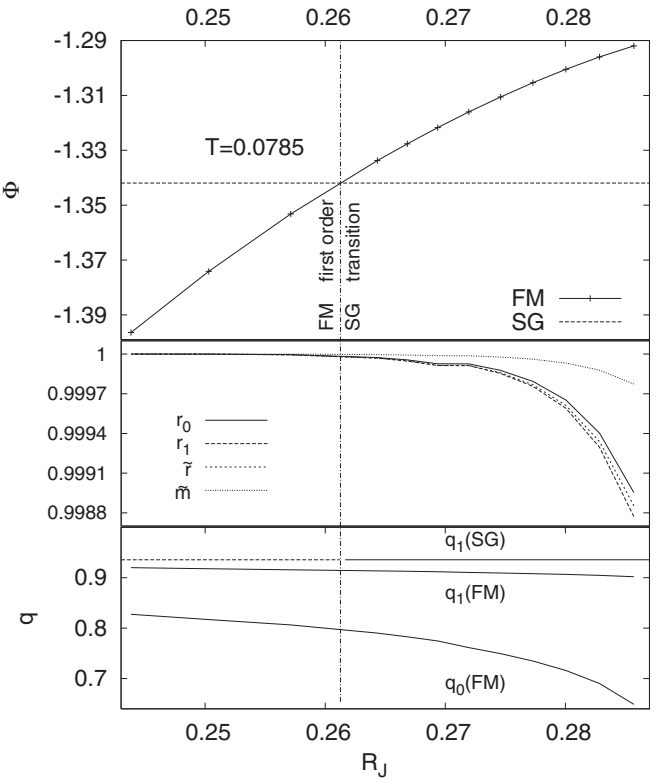

FIG. 11. Top panel panel: Free energy of the FM and SG phases vs R_J at $T = 0.0785$. As the degree of disorder increases the system undergoes a first-order phase transition from a ferromagnetic phase to a spin-glass phase. Middle panel: Order parameters r_1, r_0, and $\tilde{r}$ and the magnetization $\tilde{m}$ are shown vs R_J. Beyond the transition point their values drop to zero in the SG phase. Bottom panel: q order parameters for the FM phase and the SG phase.

VII. CONCLUSION

We have reported on an extensive theoretical treatment of the thermodynamic and dynamic phases of nonlinear waves in a random system. The approach allows us to treat nonlinearity and an arbitrary degree of disorder on the same ground and to predict the existence of complex coherent phases detailed in a specific phase diagram. The whole theoretical treatment is limited to the quenched-amplitude approximation, which allows us to capture the basic phenomenology and to demonstrate the existence of phases with a nonvanishing complexity in a variety of physical systems, specifically random lasers, finite-temperature BECs, and nonlinear optics. This approximation will be removed in future works, and novel exotic phases of light in nonlinear random systems will be detailed.

Our theoretical work shows that the interplay of nonlinearity and disorder leads to the prediction of substantially innovative physical effects, which bridge the gap between fundamental mathematical models of statistical mechanics and nonlinear waves. This allows one to identify frustration and complexity as the leading mechanisms for a coherent wave regime in nonlinear disordered systems. The natural extension of this work will be considering the quantum counterpart of the predicted transitions and the analysis of out of equilibrium nonlinear waves dynamics.

ACKNOWLEDGMENTS

The research leading to these results has received funding from the European Research Council under the European Community's Seventh Framework Program (FP7/2007-2013)/ERC Grant No. 201766 and from the Italian Ministry of Education, University and Research under the Basic Research Investigation Fund (FIRB/2008) program/CINECA Grant RBFR08M3P4, and CINECA-ISCRA10.

APPENDIX: REPLICA COMPUTATION OF THE THERMODYNAMIC PROPERTIES

The replicated partition function of the system described by the Hamiltonian $\mathcal{H}[\{\phi_j\}]$, cf. Eq. (13), reads

$$Z_J^n = \int \prod_{a=1}^{n} \prod_{j=1}^{N} d\phi_j^a \exp\left[-\beta \sum_{a=1}^{n} \mathcal{H}\left[\left\{\phi_j^a\right\}\right]\right]. \quad \text{(A1)}$$

In order to compute the free energy of the system using the replica trick, cf. Eq. (39), Eq. (A1) has to be averaged over the probability distribution of independent identically distributed random bonds:

$$P(J) \equiv \sqrt{\frac{N^3}{2\pi\sigma_J^2}} \exp\left[-N^3 \frac{(J - J_0/N^3)^2}{2\sigma_J^2}\right]. \quad \text{(A2)}$$

Equation (41) then reads

$$\overline{Z_J^n} = \int \mathcal{D}\phi \exp\left\{ N\left[\frac{\beta^2\sigma_J^2}{32} \sum_{a=1}^{n} (1 + |\tilde{R}_a(\{\phi\})|^4) + \frac{\beta^2\sigma_J^2}{16} \sum_{a<b} (|Q_{ab}(\{\phi\})|^4 + |R_{ab}(\{\phi\})|^4) + \frac{\beta J_0}{8} \sum_{a=1}^{n} |M_a(\{\phi\})|^4 \right]\right\}, \quad \text{(A3)}$$

with

$$\mathcal{D}\phi \equiv \prod_{a=1}^{n} \prod_{j=1}^{N} d\phi_j^a \quad \text{(A4)}$$

and

$$Q_{ab}(\{\phi\}) \equiv \frac{1}{N} \sum_{j=1}^{N} e^{\imath(\phi_j^a - \phi_j^b)}, \quad M_a(\{\phi\}) \equiv \frac{1}{N} \sum_{j=1}^{N} e^{\imath\phi_j^a}, \quad \text{(A5)}$$

$$R_{ab}(\{\phi\}) \equiv \frac{1}{N} \sum_{j=1}^{N} e^{\imath(\phi_j^a + \phi_j^b)}, \quad \tilde{R}_a(\{\phi\}) \equiv \frac{1}{N} \sum_{j=1}^{N} e^{2\imath\phi_j^a}, \quad \text{(A6)}$$

where we used the Euler's formula to represent the cosine and introduced abbreviations for the quantities Eqs. (A5)–(A6). We notice that the matrix Q_{ab} is Hermitian. A further step is to introduce extra parameters—that will eventually result in the order parameters identifying the various phases of the system—by means of the following identities:

$$1 = \prod_{a<b}^{1,n} N^2 \int dq_{ab} \delta[N(Q_{ab}(\{\phi\}) - q_{ab})], \quad \text{(A7)}$$

$$1 = \prod_{a<b}^{1,n} N^2 \int dr_{ab} \delta[N(R_{ab}(\{\phi\}) - r_{ab})], \quad \text{(A8)}$$

$$1 = \prod_{a=1}^{n} N^2 \int d\tilde{r}_a \delta[N(\tilde{R}_a(\{\phi\}) - \tilde{r}_a)], \quad \text{(A9)}$$

$$1 = \prod_{a=1}^{n} N^2 \int d\tilde{m}_a \delta[N(M_a(\{\phi\}) - \tilde{m}_a)], \quad \text{(A10)}$$

$$\delta[N(Q_{ab}(\{\phi\}) - q_{ab})] = \int \frac{d\lambda_{ab}}{2\pi} e^{\Re[\bar{\lambda}_{ab} N(Q_{ab}(\{\phi\}) - q_{ab})]}, \quad \text{(A11)}$$

$$\delta[N(R_{ab}(\{\phi\}) - r_{ab})] = \int \frac{d\mu_{ab}}{2\pi} e^{\Re[\bar{\mu}_{ab} N(R_{ab}(\{\phi\}) - r_{ab})]}, \quad \text{(A12)}$$

$$\delta[N(\tilde{R}_a(\{\phi\}) - \tilde{r}_a)] = \int \frac{d\tilde{\mu}_a}{2\pi} e^{\Re[\bar{\tilde{\mu}}_a N(\tilde{R}_a(\{\phi\}) - \tilde{r}_a)]}, \quad \text{(A13)}$$

$$\delta[N(M_a(\{\phi\}) - \tilde{m}_a)] = \int \frac{d\nu_a}{2\pi} e^{\Re[\bar{\nu}_a N(M_a(\{\phi\}) - \tilde{m}_a)]},$$

with $dy_{ab} = dy_{ab}^R dy_{ab}^I$. The two-index auxiliary variables q_{ab} and r_{ab}, defined for distinct couples of replicas a and b, with $a < b$, are considered in the following as elements of symmetric matrices [cf. Eqs. (A26) and (A52)], i.e., $q_{ab} = q_{ba}$ and $r_{ab} = r_{ba}$. In particular, since $Q_{ab}(\phi) = \bar{Q}_{ba}(\phi)$, Eq. (A7) implies that $q_{ab} = \bar{q}_{ab}$ are real valued.

Denoting for shortness the sets of parameters by the "vectors" $\mathbf{Q} = \{q, r, \tilde{r}, \tilde{m}\}$ and $\Lambda = \{\lambda, \mu, \tilde{\mu}, \nu\}$, this leads to

$$\overline{Z_J^n} = \int \mathcal{D}\mathbf{Q}\mathcal{D}\mathbf{\Lambda} e^{-NnG[\mathbf{Q},\mathbf{\Lambda}]}, \quad \text{(A14)}$$

$$nG[\mathbf{Q},\mathbf{\Lambda}] = nA[\mathbf{Q},\mathbf{\Lambda}] - \log Z_\phi[\mathbf{\Lambda}],$$

$$nA[\mathbf{Q},\mathbf{\Lambda}] \equiv -\frac{\beta^2\sigma_J^2}{32} \sum_{a=1}^{n} (1 + |\tilde{r}_a|^4) - \frac{\beta J_0}{8} \sum_{a=1}^{n} |\tilde{m}_a|^4 - \frac{\beta^2\sigma_J^2}{16} \sum_{a<b}^{1,n} (|q_{ab}|^4 + |r_{ab}|^4) + \sum_{a<b}^{1,n} \Re[q_{ab}\bar{\lambda}_{ab} + r_{ab}\bar{\mu}_{ab}] + \sum_{a=1}^{n} \Re[\tilde{r}_a\bar{\tilde{\mu}}_a + \tilde{m}_a\bar{\nu}_a], \quad \text{(A15)}$$

$$Z_\phi[\mathbf{\Lambda}] \equiv \int \prod_{a=1}^{n} d\phi_a e^{-\beta\mathcal{H}_{\text{eff}}[\{\phi\};\mathbf{\Lambda}]}, \quad \text{(A16)}$$

$$-\beta\mathcal{H}_{\text{eff}}[\{\phi\};\mathbf{\Lambda}] \equiv \sum_{a<b}^{1,n} \Re[e^{\imath(\phi_a - \phi_b)}\bar{\lambda}_{ab} + e^{\imath(\phi_a + \phi_b)}\bar{\mu}_{ab}] + \sum_{a=1}^{n} \Re[e^{2\imath\phi_a}\bar{\tilde{\mu}}_a + e^{\imath\phi_a}\bar{\nu}_a], \quad \text{(A17)}$$

with

$$\mathcal{D}\mathbf{Q} \equiv \prod_{a<b}^{1,n} N^4 dq_{ab} dr_{ab} \times \prod_{a=1}^{n} N^4 d\tilde{r}_a d\tilde{m}_a,$$
$$\mathcal{D}\mathbf{\Lambda} \equiv \prod_{a<b}^{1,n} \frac{d\lambda_{ab}}{2\pi}\frac{d\mu_{ab}}{2\pi} \times \prod_{a=1}^{n} \frac{d\tilde{\mu}_a}{2\pi}\frac{d\nu_a}{2\pi}.$$

The average replicated partition function integral can be estimated by the saddle-point method for large N, i.e., by approximating

$$\int \mathcal{D}[\mathbf{X}] e^{NF[\mathbf{X}]} \simeq e^{NF[\mathbf{X}_{\rm sp}]},$$
$$\frac{\partial F}{\partial X_j}\Big|_{\mathbf{X}=\mathbf{X}_{\rm sp}} = 0, \quad \forall j = 1, \ldots, \#\text{ parameters}.$$

Denoting by $\langle\cdots\rangle_{\rm eff}$ the average over the measure $e^{-\beta\mathcal{H}_{\rm eff}}$, the saddle-point equations are

$$q_{ab} = \langle e^{\imath(\phi_a-\phi_b)}\rangle_{\rm eff}; \quad \lambda_{ab} = \frac{\beta^2\sigma_J^2}{4}|q_{ab}|^2 q_{ab}; \tag{A18}$$
$$r_{ab} = \langle e^{\imath(\phi_a+\phi_b)}\rangle_{\rm eff}; \quad \mu_{ab} = \frac{\beta^2\sigma_J^2}{4}|r_{ab}|^2 r_{ab}; \tag{A19}$$
$$\forall a,b = 1,\ldots,n;\ a<b;$$
$$\tilde{r}_a = \langle e^{2\imath\phi_a}\rangle_{\rm eff}; \quad \tilde{\mu}_a = \frac{\beta^2\sigma_J^2}{8}|\tilde{r}_a|^2\tilde{r}_a \tag{A20}$$
$$\tilde{m}_a = \langle e^{\imath\phi_a}\rangle_{\rm eff}; \quad \nu_a = \frac{\beta J_0}{2}|\tilde{m}_a|^2\tilde{m}_a; \tag{A21}$$
$$\forall a = 1,\ldots,n.$$

The diagonal values of the overlap matrices are set to zero. Eventually, according to Eq. (39), one has

$$\beta\Phi = -\frac{1}{N}\lim_{n\to 0}\frac{e^{-nNG[\mathbf{Q}_{\rm sp},\mathbf{\Lambda}_{\rm sp}]}-1}{n} = \lim_{n\to 0} G[\mathbf{Q}_{\rm sp},\mathbf{\Lambda}_{\rm sp}]. \tag{A22}$$

The parameters with a single-replica index turn out not to depend on the specific replica. Indeed, Eqs. (A20)–(A21) might in principle be obtained by perturbing the original Hamiltonian with a small field coupled to a local function of the planar, XY, spins $S = e^{\imath\phi}$, independently from the possible introduction of replicas.

If the perturbation is $-k\sum_{j=1}^{N} S_j^2$, we obtain

$$\tilde{r}_d = -\frac{1}{N}\frac{\partial\overline{\log Z_J}}{\partial k} = \frac{1}{N}\sum_{j=1}^{N}\overline{S_j^2} \to \overline{\langle S^2\rangle} \quad (\text{as } N\to\infty), \tag{A23}$$

which is valid *for any* replica and, therefore independent from any replica index: $\tilde{r}_d = \tilde{r}_a, \forall a = 1,\ldots,n$. In the replica formalism, the same quantity can equivalently be written as

$$\tilde{r}_d = -\lim_{n\to 0}\frac{1}{nN}\frac{\partial\overline{Z_J^n}}{\partial k} = \lim_{n\to 0}\frac{1}{n}\sum_{a=1}^{n}\tilde{r}_a,$$

and this trivially leads to the identification

$$\tilde{r}_a = \lim_{n\to 0}\frac{1}{n}\sum_{a=1}^{n}\tilde{r}_a = \tilde{r}_d. \tag{A24}$$

Similarly, perturbing Eq. (13) with $-h\sum_{j=1}^{N} S_j$, we get

$$\tilde{m} = -\frac{1}{N}\frac{\partial\overline{\log Z_J}}{\partial h} = \frac{1}{N}\sum_{j=1}^{N}\overline{S_j},$$
$$\tilde{m} = -\lim_{n\to 0}\frac{1}{nN}\frac{\partial\overline{Z_J^n}}{\partial h} = \lim_{n\to 0}\frac{1}{n}\sum_{a=1}^{n}\tilde{m}_a. \tag{A25}$$

Though no external ad hoc perturbation can be applied to the Hamiltonian Eq. (A17) to reproduce two-index quantities, the same symmetry should apply, since all replicas of the original problem were introduced in the same way: the system is symmetric under replica exchange. This is called the replica symmetric (RS) ansatz:

$$q_{ab} = q\forall a\neq b; \quad r_{ab} = r\forall a\neq b \tag{A26}$$

A. Replica symmetric ansatz

In this ansatz, Eqs. (A16) and (A17) become

$$Z_\phi^{\rm RS} = \int\prod_{a=1}^{n} d\phi_a e^{-\beta\mathcal{H}_{\rm eff}[\{\phi_a\}]}, \tag{A27}$$

$$\beta\mathcal{H}_{\rm eff} = \frac{\lambda^R}{2}\left(n - \left|\sum_{a=1}^{n} e^{\imath\phi_a}\right|^2\right) - \Re\left[\frac{\bar{\mu}}{2}\left(\sum_{a=1}^{n} e^{\imath\phi_a}\right)^2 + \left(\tilde{\bar{\mu}} - \frac{\bar{\mu}}{2}\right)\sum_{a=1}^{n} e^{2\imath\phi} + \bar{\nu}\sum_{a=1}^{n} e^{\imath\phi}\right]. \tag{A28}$$

The second term on the right-hand side can be rewritten as

$$\Re\left[\frac{\bar{\mu}}{2}\left(\sum_{a=1}^{n} e^{\imath\phi_a}\right)^2\right] = \Re\left[\frac{\mu}{2}\left(\sum_{a=1}^{n} e^{-\imath\phi_a}\right)^2\right] = \Re\left[\frac{1}{4}\left(\sqrt{\bar{\mu}}\sum_{a=1}^{n} e^{\imath\phi_a} + \sqrt{\mu}\sum_{a=1}^{n} e^{-\imath\phi_a}\right)^2\right] - \frac{|\mu|}{2}\left|\sum_{a=1}^{n} e^{\imath\phi_a}\right|^2. \tag{A29}$$

The squared terms in the exponent of the integrand can be linearized by using

$$e^{|w|^2/2} = \int\frac{d\zeta^R d\zeta^I}{2\pi} e^{-|\zeta|^2/2} e^{\Re(\bar{\zeta}w)}, \tag{A30}$$
$$e^{w_R^2/2} = \int\frac{dx}{\sqrt{2\pi}} e^{-x^2/2} e^{xw_R}, \tag{A31}$$

thus yielding

$$Z_\phi^{\rm RS} = \int \mathcal{D}p(x)\mathcal{D}p(\zeta^R)\mathcal{D}p(\zeta^I)\left[\int_0^{2\pi} d\phi e^{\mathcal{L}(\phi;x,\zeta)}\right]^n, \quad \text{(A32)}$$

$$\mathcal{L}(\phi;x,\zeta) \equiv \Re\Big[e^{\imath\phi}(\bar\zeta\sqrt{\lambda-|\mu|}+x\sqrt{2\bar\mu}+\bar\nu) + e^{2\imath\phi}\left(\bar{\tilde\mu}-\frac{\bar\mu}{2}\right)\Big] \quad \text{(A33)}$$

$$\mathcal{D}p(w) = \frac{dw}{\sqrt{2\pi}}e^{-w^2/2}. \quad \text{(A34)}$$

The replicated free energy eventually reads

$$\begin{aligned}\beta\Phi = &-\frac{\beta^2\sigma_J^2}{32}[1-|q|^4-|r|^4+|\tilde r|^4]\\ &-\frac{\beta J_0}{8}|\tilde m|^4+\frac{\lambda^R}{2}(1-q^R)-\frac{1}{2}\Re[\bar\mu r-2\bar{\tilde\mu}\tilde r-2\bar\nu\tilde m]\\ &-\int\mathcal{D}p(x)\mathcal{D}p(\zeta^R)\mathcal{D}p(\zeta^I)\log\int_0^{2\pi}d\phi e^{\mathcal{L}(\phi;x,\zeta)}.\end{aligned} \quad \text{(A35)}$$

Deriving with respect to the Q parameter we obtain the specification of Eqs. (A18)–(A21) for the replica overlap parameters q and r and for $\tilde r$ and $\tilde m$:

$$\lambda = \frac{\beta^2\sigma_J^2}{4}q^3, \quad \text{(A36)}$$

$$\begin{aligned}\mu &= \frac{\beta^2\sigma_J^2}{4}|r|^2 r,\\ \tilde\mu &= \frac{\beta^2\sigma_J^2}{8}|\tilde r|^2\tilde r, \quad \text{(A37)}\\ \nu &= \frac{\beta J_0}{2}|\tilde m|^2\tilde m.\end{aligned}$$

Taking the derivative of $\beta\Phi$ in Eq. (A35)with respect to $\tilde\mu$ and ν we obtain

$$\tilde r_d = \langle\langle e^{2\imath\phi}\rangle_{\mathcal{L}}\rangle_{x,\zeta}, \quad \text{(A38)}$$

$$\tilde m = \langle\langle e^{\imath\phi}\rangle_{\mathcal{L}}\rangle_{x,\zeta}, \quad \text{(A39)}$$

where we define

$$\langle\cdots\rangle_{\mathcal{L}} \equiv \frac{\int_0^{2\pi}d\phi\ldots e^{\mathcal{L}(\phi;x,\zeta)}}{\int_0^{2\pi}d\phi e^{\mathcal{L}(\phi;x,\zeta)}}. \quad \text{(A40)}$$

Deriving G with respect to λ and μ and equating to zero we obtain

$$q^R = \left\langle c_{\mathcal{L}}^2+s_{\mathcal{L}}^2\right\rangle_{x,\zeta}, \quad \text{(A41)}$$

$$\begin{aligned}r &= \left\langle c_{\mathcal{L}}^2-s_{\mathcal{L}}^2+2\imath c_{\mathcal{L}}s_{\mathcal{L}}\right\rangle_{x,\zeta},\\ c_{\mathcal{L}} &\equiv \langle\cos\phi\rangle_{\mathcal{L}}, \qquad s_{\mathcal{L}} \equiv \langle\sin\phi\rangle_{\mathcal{L}},\end{aligned} \quad \text{(A42)}$$

after having integrated by part in the Gaussian measures. To help the nonexpert reader to easily derive the self-consistency equations we exemplify the calculation of Eq. (A18):

$$2\frac{\partial G}{\partial\lambda^R} = 0 = 1-q^R - \langle(\zeta^R c_{\mathcal{L}}+\zeta^I s_{\mathcal{L}})\rangle_{x,\zeta}/\sqrt{\lambda^R-|\mu|}. \quad \text{(A43)}$$

The latter term can be simplified by integrating by part,

$$\int_{-\infty}^{\infty}\mathcal{D}p(y)yF(y) = \int_{-\infty}^{\infty}\mathcal{D}p(y)\frac{\partial F(y)}{\partial y}, \quad \text{(A44)}$$

with $y=\zeta^R,\zeta^I$ in Eq. (A44), yielding

$$\langle\zeta^R c_{\mathcal{L}}+\zeta^I s_{\mathcal{L}}\rangle_{x,\zeta} = \sqrt{\lambda^R-|\mu|}\times\left\langle\cos^2\phi-c_{\mathcal{L}}^2+\sin^2\phi-s_{\mathcal{L}}^2\right\rangle_{x,\zeta}. \quad \text{(A45)}$$

The self-consistency equation can thus be rewritten as [cf. Eq. (51)],

$$\begin{aligned}1-q^R &= 1-\left\langle c_{\mathcal{L}}^2+s_{\mathcal{L}}^2\right\rangle_{x,\zeta},\\ q^R &= \left\langle c_{\mathcal{L}}^2\right\rangle_{x,\zeta}+\left\langle s_{\mathcal{L}}^2\right\rangle_{x,\zeta}.\end{aligned}$$

We recall that since q_{ab} is real, and so is λ_{ab}, cf. Eq. (A18), in the RS ansatz equations $q^I=\lambda^I=0$.

Before deriving Eq. (A44), we rewrite the part of Eq. (A33) involving the integrating variable x as

$$\Re[e^{\imath\phi}x\sqrt{2\bar\mu}] = x\sqrt{|\mu|}\left(\cos\phi\sqrt{1+\frac{\mu^R}{|\mu|}}+\sin\phi\sqrt{1-\frac{\mu^R}{|\mu|}}\right). \quad \text{(A46)}$$

In determining the above expression one can use, e.g., the trigonometric law of tangents to yield

$$\frac{1}{2}\arctan\frac{\mu^I}{\mu^R} = \arctan\sqrt{\frac{1-\mu^R/|\mu|}{1+\mu^R/|\mu|}} \quad \text{(A47)}$$

and the relationships between trigonometric and inverse trigonometric functions:

$$\begin{aligned}\sin[\arctan(\theta)] &= \frac{\theta}{\sqrt{1+\theta^2}},\\ \cos[\arctan(\theta)] &= \frac{1}{\sqrt{1+\theta^2}}.\end{aligned}$$

Using Eq. (A46), together with Eqs. (A38) and (A41), we have

$$2\frac{\partial G}{\partial\mu^R} = 0 = r_d^R-r^R+\frac{\mu^R}{|\mu|}(1-q) - \left\langle x\left(c_{\mathcal{L}}\sqrt{1+\frac{\mu^R}{|\mu|}}+s_{\mathcal{L}}\sqrt{1-\frac{\mu^R}{|\mu|}}\right)\right\rangle_{x,\zeta}/\sqrt{|\mu|}. \quad \text{(A48)}$$

Integrating by part with Eq. (A44), $y=x$, we find

$$\left\langle x\left(c_{\mathcal{L}}\sqrt{1+\frac{\mu^R}{|\mu|}}+s_{\mathcal{L}}\sqrt{1-\frac{\mu^R}{|\mu|}}\right)\right\rangle_{x,\zeta} = \sqrt{|\mu|}\left\langle\left[\langle\cos 2\phi\rangle_{\mathcal{L}}-c_{\mathcal{L}}^2+s_{\mathcal{L}}^2+\frac{\mu^R}{|\mu|}\left(1-c_{\mathcal{L}}^2-s_{\mathcal{L}}^2\right)\right]\right\rangle_{x,\zeta}, \quad \text{(A49)}$$

and eventually one obtains the real part of Eq. (A42). The imaginary part of the self-consistency equation for r is analogously determined from $\frac{\partial G}{\partial\mu^I}=0$.

Above a given critical temperature (depending on J_0) the solution to Eqs. (A38), (A39), (A41), and (A42) is paramagnetic, i.e., $q = r = \tilde{m} = \tilde{r} = 0$, and the free energy is

$$\beta\Phi_{\rm PM} = -\frac{\bar{\beta}^2}{32} - \log 2\pi. \tag{A50}$$

Below $T_c(J_0)$, depending on the value of J_0 the solution can either be ferromagnetic $\tilde{m} \neq 0$ or spin-glass $\tilde{m} = 0$. The latter solutions are, however, not stable against fluctuations in the space of replica overlaps[105] and, thus, we have to try an ansatz different from Eq. (A26) to provide a self-consistent thermodynamics.

B. One step of replica symmetry breaking

In order to obtain a thermodynamically consistent result the symmetry cannot be conserved. We are in the presence of a spontaneous RSB. The way to break the symmetry must be *a priori* hypothesized, since there has been found, so far, no way to deduce it. The correct way to express the elements of the overlap matrices is called the Parisi ansatz[77,78] and, depending on the kind of system, can consist of one or more RSBs. According to what happens in other spin models with p-body quenched random interactions (p being larger than 2), the right ansatz for the matrices of our model is the 1RSB, that is, we have an $n \times n$ matrix divided in square blocks of $m \times m$ elements:

$$q_{ab} = q_1; \quad r_{ab} = r_1, \quad \text{if } I\left(\frac{a}{m}\right) = I\left(\frac{b}{m}\right); \tag{A51}$$

$$q_{ab} = q_0; \quad r_{ab} = r_0, \quad \text{if } I\left(\frac{a}{m}\right) \neq I\left(\frac{b}{m}\right). \tag{A52}$$

For instance, for $n = 6$ and $m = 3$,

$$q_{(\alpha\beta)} = \begin{pmatrix} 0 & q_1 & q_1 & q_0 & q_0 & q_0 \\ q_1 & 0 & q_1 & q_0 & q_0 & q_0 \\ q_1 & q_1 & 0 & q_0 & q_0 & q_0 \\ q_0 & q_0 & q_0 & 0 & q_1 & q_1 \\ q_0 & q_0 & q_0 & q_1 & 0 & q_1 \\ q_0 & q_0 & q_0 & q_1 & q_1 & 0 \end{pmatrix}.$$

The one-replica index observables are instead still RS, as exemplified in Eqs. (A23)–(A25). Now, let us write the "vectorial" replica index:

$$a \to \mathbf{a} = (a_1, a_2),$$
$$\phi_a \to \phi_{\mathbf{a}} = \phi_{a_1,a_2},$$
$$\sum_{a=1}^{n} O_a = \sum_{a_1=1}^{n/m} \sum_{a_2=1}^{m} O_{a_1 a_2}.$$

Take a 1RSB matrix K_{ab} and two replicated observables g_a and h_a. The following expressions hold for the sum of a generic product:

$$\begin{aligned} 2\sum_{a<b} K_{ab} g_a h_b &= K_{ab} g_a h_b \\ &= K_1 \sum_{a_1=1}^{n/m} \sum_{a_2 \neq b_2}^{1,m} g_{a_1 a_2} h_{a_1 b_2} + K_0 \sum_{a_1 \neq b_1}^{1,n/m} \sum_{a_2 b_2}^{1,m} g_{a_1 a_2} h_{b_1 b_2} \\ &= K_1 \sum_{a_1=1}^{n/m} \sum_{a_2,b_2}^{1,m} g_{a_1 a_2} h_{a_1 b_2} - K_1 \sum_{a_1=1}^{n/m} \sum_{a_2=1}^{m} g_{a_1 a_2} h_{a_1 a_2} \\ &\quad + K_0 \sum_{a_1,b_1}^{1,n/m} \sum_{a_2,b_2}^{1,m} g_{a_1 a_2} h_{b_1 b_2} - K_0 \sum_{a_1=1}^{n/m} \sum_{a_2,b_2}^{1,m} g_{a_1 a_2} h_{a_1 b_2}. \end{aligned} \tag{A53}$$

If we take $g = \bar{h}$,

$$\begin{aligned} 2\sum_{a<b} K_{ab} |g_a|^2 &= (K_1 - K_0) \sum_{a_1=1}^{n/m} \left| \sum_{a_2=1}^{m} g_{a_1 a_2} \right|^2 \\ &\quad - K_1 \sum_{a=1}^{n} |g_a|^2 + K_0 \left| \sum_{a=1}^{n} g_a \right|^2. \end{aligned} \tag{A54}$$

If we take $g = h$,

$$\begin{aligned} 2\sum_{a<b} K_{ab} g_{ab}^2 &= (K_1 - K_0) \sum_{a_1=1}^{n/m} \left(\sum_{a_2=1}^{m} g_{a_1 a_2} \right)^2 \\ &\quad - K_1 \sum_{a=1}^{n} (g_a)^2 + K_0 \left(\sum_{a=1}^{n} g_a \right)^2. \end{aligned} \tag{A55}$$

Substituting into Eqs. (A16) and (A17) both Eq. (A54)—with $K = \bar{\lambda}$ and $g = \bar{h} = e^{\imath\phi}$—and Eq. (A55)—with $K = \bar{\mu}$ and $g = h = e^{\imath\phi}$—one obtains

$$Z_\phi^{\rm 1RSB} = \int \prod_{a_1=1}^{n/m} \prod_{a_2=1}^{m} d\phi_{a_1 a_2} e^{-\beta \mathcal{H}_{\rm eff}[\{\phi_{a_1 a_2}\}]}, \tag{A56}$$

$$\begin{aligned} \beta\mathcal{H}_{\rm eff} = \Re\Bigg[&- \frac{\Delta\bar{\lambda}}{2} \sum_{a_1=1}^{n/m} \left| \sum_{a_2=1}^{m} e^{\imath\phi_{a_1 a_2}} \right|^2 - n\frac{\bar{\lambda}_1}{2} + \frac{\bar{\lambda}_0}{2} \left| \sum_{a=1}^{n} e^{\imath\phi_a} \right|^2 \\ &+ \frac{\Delta\bar{\mu}}{2} \sum_{a_1=1}^{n/m} \left(\sum_{a_2=1}^{m} e^{\imath\phi_{a_1 a_2}} \right)^2 - \frac{\bar{\mu}_1}{2} \sum_{a=1}^{n} e^{2\imath\phi_a} \\ &+ \frac{\bar{\mu}_0}{2} \left(\sum_{a=1}^{n} e^{\imath\phi_a} \right)^2 + \bar{\tilde{\mu}} \sum_{a=1}^{n} e^{2\imath\phi_a} + \bar{\nu} \sum_{a=1}^{n} e^{\imath\phi_a} \Bigg], \end{aligned} \tag{A57}$$

$$\Delta\bar{\lambda} = \bar{\lambda}_1 - \bar{\lambda}_0, \qquad \Delta\bar{\mu} = \bar{\mu}_1 - \bar{\mu}_0.$$

Using the identities

$$\Re[(ab)^2] = \Re[(\bar{a}\bar{b})^2] = \Re\left[\frac{(ab + \bar{a}\bar{b})^2}{2} - |a||b|\right], \tag{A58}$$

$$e^{A_R |g|^2/2} = \int \frac{d\zeta_R d\zeta_I}{2\pi} e^{-|\zeta|^2/2} e^{\Re[\bar{\zeta}\sqrt{A_R} g]}, \tag{A59}$$

$$e^{\Re[Ag^2]/2} = \int_{-\infty}^{\infty} \frac{dx}{\sqrt{2\pi}} e^{-x^2/2} e^{x\Re[\sqrt{A} g]}, \tag{A60}$$

where A is complex and A_R is real, we can linearize the dependence on $e^{\imath\phi}$ in the partition function Eq. (A56) using Gaussian integral expressions:

$$\Re\left[\frac{\bar{\lambda}_0}{2}\left|\sum_{a=1}^{n} e^{\imath\phi_a}\right|^2 + \frac{\bar{\mu}_0}{2}\left(\sum_{a=1}^{n} e^{\imath\phi_a}\right)^2\right] = \log\int \mathcal{D}[\mathbf{0}]\exp\Re\left[\bar{\zeta}_0\sqrt{\lambda_0^R - |\mu_0|}\sum_{a=1}^{n} e^{\imath\phi_a} + \frac{x_0}{\sqrt{2}}\left(\sqrt{\bar{\mu}_0}\sum_{a=1}^{n} e^{\imath\phi_a} + \sqrt{\mu_0}\sum_{a=1}^{n} e^{-\imath\phi_a}\right)\right], \quad \text{(A61)}$$

$$\Re\left[\frac{\Delta\bar{\lambda}}{2}\left|\sum_{a_2=1}^{m} e^{\imath\phi_{a_1 a_2}}\right|^2 + \frac{\Delta\bar{\mu}}{2}\left(\sum_{a_2=1}^{m} e^{\imath\phi_{a_1 a_2}}\right)^2\right] = \log\int \mathcal{D}[\mathbf{1}]\exp\Re\left[\bar{\zeta}_1\sqrt{\Delta\lambda^R - |\Delta\mu|}\sum_{a_2=1}^{m} e^{\imath\phi_{a_1 a_2}} + \frac{x_1}{\sqrt{2}}\left(\sqrt{\Delta\bar{\mu}}\sum_{a_2=1}^{m} e^{\imath\phi_{a_1 a_2}} + \sqrt{\Delta\mu}\sum_{a_2=1}^{m} e^{-\imath\phi_{a_1 a_2}}\right)\right], \quad \text{(A62)}$$

where we defined the following Gaussian measures:

$$\mathcal{D}p\left(\zeta_k^{R,I}\right) = \frac{d\zeta_k^{R,I}}{\sqrt{2\pi}} e^{-(\zeta_k^{R,I})^2/2}, \quad \text{(A63)}$$

$$\mathcal{D}p(x_k) = \frac{dx_k}{\sqrt{2\pi}} e^{-x_k^2/2}, \quad \text{(A64)}$$

$$\mathcal{D}[\mathbf{k}] = \mathcal{D}p\left(\zeta_k^R\right)\mathcal{D}p\left(\zeta_k^I\right)\mathcal{D}p\left(x_k\right). \quad \text{(A65)}$$

Equation (A56) becomes

$$Z_\phi^{\text{1RSB}} = e^{-n\lambda_1^R/2} \times \int \mathcal{D}[\mathbf{0}]\prod_{a_1=1}^{n/m}\left\{\int \mathcal{D}[\mathbf{1}]\int \mathcal{D}\phi\prod_{a_2=1}^{m} e^{\mathcal{L}(\phi_{a_1 a_2};\mathbf{0},\mathbf{1})}\right\}, \quad \text{(A66)}$$

$$\mathcal{L}(\psi;\mathbf{0},\mathbf{1}) \equiv \Re\left[e^{\imath\psi}\left(\bar{\zeta}_1\sqrt{\Delta\lambda^R - |\Delta\mu|} + \bar{\zeta}_0\sqrt{\lambda_0^R - |\mu_0|} + 2x_1\sqrt{\frac{\Delta\bar{\mu}}{2}} + 2x_0\sqrt{\frac{\bar{\mu}_0}{2}} + \bar{\nu}\right) + e^{2\imath\psi}\left(\bar{\tilde{\mu}} - \frac{\bar{\mu}_1}{2}\right)\right], \quad \text{(A67)}$$

cf. Eq. (46). In the $n \to 0$ limit the "phase contribution" to the replicated free energy is

$$-\lim_{n\to 0}\frac{1}{n}\log Z_\phi^{\text{1RSB}} = \frac{\lambda_1^R}{2} - \frac{1}{m}\int \mathcal{D}[\mathbf{0}]\log\int \mathcal{D}[\mathbf{1}]\left[\int d\phi e^{\mathcal{L}(\phi;\mathbf{0},\mathbf{1})}\right]^m, \quad \text{(A68)}$$

and the free energy is

$$\begin{aligned}\beta\Phi &= \lim_{n\to 0} G_{\text{1RSB}}[\mathbf{Q}_{\text{sp}};\mathbf{\Lambda}_{\text{sp}}] \\ &= -\frac{\beta^2\sigma_J^2}{32}[1-(1-m)(|q_1|^4+|r_1|^4) - m(|q_0|^4+|r_0|^4) + |\tilde{r}|^4] \\ &\quad - \frac{1}{2}\Re[(1-m)(\bar{\lambda}_1 q_1 + \bar{\mu}_1 r_1) + m(\bar{\lambda}_0 q_0 + \bar{\mu}_0 r_0)] \\ &\quad - \frac{\beta J_0}{8}|\tilde{m}|^4 + \Re[\bar{\tilde{\mu}}\tilde{r} + \bar{\nu}\tilde{m}] - \lim_{n\to 0}\frac{1}{n}\log Z_\phi^{\text{1RSB}}.\end{aligned} \quad \text{(A69)}$$

Saddle-point equations. Deriving G/n with respect to the parameters, we obtain the 12 self-consistency equations determining the order parameter values at a given external pumping intensity and amount of disorder.

(i) Deriving with respect to the Q parameter we obtain the specification of Eqs. (A18)–(A21) for each 1RSB replica matrix sector and for $\tilde{r}$ and $\tilde{m}$ [cf. Eqs. (49) and (50)],

$$\lambda_{0,1} = \frac{\beta^2\sigma_J^2}{4} q_{0,1}|q_{0,1}|^2, \quad \text{(A70)}$$

$$\mu_{0,1} = \frac{\beta^2\sigma_J^2}{4}|r_{0,1}|^2 r_{0,1}, \quad \text{(A71)}$$

$$\tilde{\mu} = \frac{\beta^2\sigma_J^2}{8}|\tilde{r}|^2\tilde{r}, \quad \text{(A72)}$$

$$\nu = \frac{\beta J_0}{2}|\tilde{m}|^2\tilde{m}. \quad \text{(A73)}$$

(ii) Deriving with respect to $\tilde{\mu}$ and ν we obtain Eqs. (55), where we define

$$\langle\ldots\rangle_{\mathcal{L}} \equiv \frac{\int_0^{2\pi} d\phi\ldots e^{\mathcal{L}(\phi;\mathbf{0},\mathbf{1})}}{\int_0^{2\pi} d\phi e^{\mathcal{L}(\phi;\mathbf{0},\mathbf{1})}}, \quad \text{(A74)}$$

$$c_{\mathcal{L}} \equiv \langle\cos\phi\rangle_{\mathcal{L}}, \quad s_{\mathcal{L}} \equiv \langle\sin\phi\rangle_{\mathcal{L}}. \quad \text{(A75)}$$

(iii) Deriving G with respect to $\lambda_{0,1}$ and $\mu_{0,1}$ and equating to zero we obtain Eqs. (51)–(54), after having integrated by part in the Gaussian measures. To help the nonexpert reader to easily derive the self-consistency equations we exemplify the calculation of Eq. (51):

$$2\frac{\partial G}{\partial\lambda_1^R} = 0 = 1 - (1-m)q_1^R - \int \mathcal{D}[\mathbf{0}]\left\langle\zeta_1^R c_{\mathcal{L}} + \zeta_1^I s_{\mathcal{L}}\right\rangle_m / \sqrt{\Delta\lambda^R - |\Delta\mu|}. \quad \text{(A76)}$$

The latter term can be simplified by integrating by part

$$\int_{-\infty}^{\infty} \mathcal{D}p(y) y F(y) = \int_{-\infty}^{\infty} \mathcal{D}p(y) \frac{\partial F(y)}{\partial y}, \qquad \text{(A77)}$$

with $y = \zeta_1^R, \zeta_1^I$ in Eq. (A77), yielding

$$\left\langle \zeta_1^R c_{\mathcal{L}} + \zeta_1^I s_{\mathcal{L}} \right\rangle_m = \sqrt{\Delta\lambda^R - |\Delta\mu|} \times \left\langle \cos^2\phi - (1-m)c_{\mathcal{L}}^2 + \sin^2\phi - (1-m)s_{\mathcal{L}}^2 \right\rangle_m. \qquad \text{(A78)}$$

The self-consistency equation can thus be rewritten as [cf. Eq. (51)]

$$1 - (1-m)q_1^R = 1 - (1-m)\int \mathcal{D}[\mathbf{0}] \left\langle c_{\mathcal{L}}^2 + s_{\mathcal{L}}^2 \right\rangle_m,$$
$$q_1^R = \left\langle \left\langle c_{\mathcal{L}}^2 \right\rangle_m \right\rangle_0 + \left\langle \left\langle s_{\mathcal{L}}^2 \right\rangle_m \right\rangle_0. \qquad \text{(A79)}$$

Equations (52)–(54) are analogously derived. We notice that, since from the equations $\partial G/\partial\lambda_{0,1}^I = 0$ one obtains $q_{0,1}^I = 0$, the values of the q overlap are real valued and so are the values of λ.

*claudio.conti@roma1.infn.it
†luca.leuzzi@cnr.it

[1] R. T. Scalettar, G. G. Batrouni, and G. T. Zimanyi, Phys. Rev. Lett. **66**, 3144 (1991).
[2] T. Schulte, S. Drenkelforth, J. Kruse, W. Ertmer, J. Arlt, K. Sacha, J. Zakrzewski, and M. Lewenstein, Phys. Rev. Lett. **95**, 170411 (2005).
[3] P. Lugan, D. Clément, P. Bouyer, A. Aspect, M. Lewenstein, and L. Sanchez-Palencia, Phys. Rev. Lett. **98**, 170403 (2007).
[4] T. Schwartz, G. Bartal, S. Fishman, and M. Segev, Nature (London) **446**, 52 (2007).
[5] G. Roati, C. D'Errico, L. Fallani, M. Fattori, C. Fort, M. Zaccanti, G. Modugno, M. Modugno, and M. Inguscio, Nature (London) **453**, 895 (2008).
[6] J. Billy, V. Josse, Z. Zuo, A. Bernard, B. Hambrecht, P. Lugan, D. Clement, L. Sanchez-Palencia, P. Bouyer, and A. Aspect, Nature (London) **453**, 891 (2008).
[7] M. White, M. Pasienski, D. McKay, S. Q. Zhou, D. Ceperley, and B. DeMarco, Phys. Rev. Lett. **102**, 055301 (2009).
[8] G. Modugno, Rep. Prog. Phys. **73**, 102401 (2010).
[9] C. Conti, L. Angelani, and G. Ruocco, Phys. Rev. A **75**, 033812 (2007).
[10] I. V. Shadrivov, K. Y. Bliokh, Y. P. Bliokh, V. Freilikher, and Y. S. Kivshar, Phys. Rev. Lett. **104**, 123902 (2010).
[11] D. S. Wiersma, Nat. Phys. **4**, 359 (2008).
[12] M. Bamba, S. Pigeon, and C. Ciuti, Phys. Rev. Lett. **104**, 213604 (2010).
[13] U. Bertolozzo, S. Residori, and P. Sebbah, Phys. Rev. Lett. **106**, 103903 (2011).
[14] J. D. Bodyfelt, T. Kottos, and B. Shapiro, Phys. Rev. Lett. **104**, 164102 (2010).
[15] T. Bienaimé, S. Bux, E. Lucioni, P. W. Courteille, N. Piovella, and R. Kaiser, Phys. Rev. Lett. **104**, 183602 (2010).
[16] C. Conti, Phys. Rev. E **72**, 066620 (2005).
[17] C. Conti, M. Peccianti, and G. Assanto, Opt. Lett. **31**, 2030 (2006).
[18] V. Folli and C. Conti, Phys. Rev. Lett. **104**, 193901 (2010).
[19] S. E. Skipetrov, Phys. Rev. E **67**, 016601 (2003).
[20] O. Zaitsev and L. Deych, J. Opt. **12**, 024001 (2010).
[21] H. Cao, Waves in Random Media and Complex Media **13**, R1 (2003).
[22] H. E. Tureci, L. Ge, S. Rotter, and A. D. Stone, Science **320**, 643 (2008).
[23] K. L. van der Molen, A. P. Mosk, and A. Lagendijk, Phys. Rev. A **74**, 053808 (2006).
[24] R. G. S. El-Dardiry, A. P. Mosk, O. L. Muskens, and A. Lagendijk, Phys. Rev. A **81**, 043830 (2010).
[25] C. Conti, M. Leonetti, A. Fratalocchi, L. Angelani, and G. Ruocco, Phys. Rev. Lett. **101**, 143901 (2008).
[26] R. Weill, B. Levit, A. Bekker, O. Gat, and B. Fischer, Opt. Express **18**, 16520 (2010).
[27] R. Weill, B. Fischer, and O. Gat, Phys. Rev. Lett. **104**, 173901 (2010).
[28] P. Suret, S. Randoux, H. R. Jauslin, and A. Picozzi, Phys. Rev. Lett. **104**, 054101 (2010).
[29] U. Bortolozzo, J. Laurie, S. Nazarenko, and S. Residori, J. Opt. Soc. Am. B **26**, 2280 (2009).
[30] S. K. Turitsyn, S. A. Babin, A. E. El-Taher, P. Harper, D. V. Churkin, S. I. Kablukov, J. D. Ania-Castanon, V. Karalekas, and E. V. Podivilov, Nat. Photon **4**, 231 (2010).
[31] H. A. Haus, IEEE J. Quantum Electron. **6**, 1173 (2000).
[32] L. Leuzzi, C. Conti, V. Folli, L. Angelani, and G. Ruocco, Phys. Rev. Lett. **102**, 083901 (2009).
[33] S. Kirkpatrick and B. Selman, Science **264**, 1297 (1994).
[34] R. Monasson, R. Zecchina, S. Kirkpatrick, B. Selman, and L. Troyansky, Nature (London) **400**, 133 (1999).
[35] M. Mézard, G. Parisi, and R. Zecchina, Science **297**, 812 (2002).
[36] M. Mézard and A. Montanari, *Information, Physics, and Computation* (Oxford University Press, Oxford, 2009).
[37] G. Akguc and L. E. Reichl, Phys. Rev. E **64**, 056221 (2001).
[38] N. M. Makarov and Y. V. Tarasov, J. Phys. Condens. Matter **10**, 1523 (1998).
[39] D. Boese, M. Lischka, and L. E. Reichl, Phys. Rev. B **61**, 5632 (2000).
[40] C. Conti and A. Fratalocchi, Nat. Phys. **4**, 794 (2008).
[41] H. A. Haus, *Waves and Fields in Optoelectronics* (Prentice-Hall, Englewood Cliffs, NJ, 1984).
[42] K. Sakoda, *Optical Properties of Photonic Crystals* (Springer-Verlag, Berlin, 2001).
[43] G. Hackenbroich, C. Viviescas, B. Elattari, and F. Haake, Phys. Rev. Lett. **86**, 5262 (2001).
[44] G. Hackenbroich, C. Viviescas, and F. Haake, Phys. Rev. A **68**, 063805 (2003).
[45] L. Angelani, C. Conti, G. Ruocco, and F. Zamponi, Phys. Rev. Lett. **96**, 065702 (2006).
[46] L. Angelani, C. Conti, G. Ruocco, and F. Zamponi, Phys. Rev. B **74**, 104207 (2006).
[47] A. Yariv, *Quantum Electronics* (Saunders College, San Diego, 1991).
[48] W. E. Lamb, Phys. Rev. **134**, A1429 (1964).

[49]M. Weigt, R. White, H. Szurmant, J. Hoch, and T. Hwa, Proc. Natl. Acad. Sci. USA **106**, 67 (2009).
[50]T. Mora, A. Walczak, W. Bialek, C. Callan, and G. Curtis Jr., Proc. Natl. Acad. Sci. USA **107**, 5405 (2010).
[51]P. Meystre and M. Sargent III, *Elements of Quantum Optics* (Springer, New York, 1998).
[52]D. S. Wiersma and S. Cavalieri, Nature (London) **414**, 708 (2001).
[53]M. Leonetti and C. Conti, J. Opt. Soc. Am. **27**, 1446 (2010).
[54]F. Dalfovo, S. Giorgini, L. Pitaevskii, and S. Stringari, Rev. Mod. Phys. **71**, 463 (1999).
[55]H. Stoof, J. Low Temp. Phys. **114**, 11 (1999).
[56]R. A. Duine and H. T. C. Stoof, Phys. Rev. A **65**, 013603 (2001).
[57]R. A. Duine, B. W. A. Leurs, and H. T. C. Stoof, Phys. Rev. A **69**, 053623 (2004).
[58]T. M. Lifshitz, Adv. Phys. **13**, 483 (1964).
[59]M. P. A. Fisher, P. B. Weichman, G. Grinstein, and D. S. Fisher, Phys. Rev. B **40**, 546 (1989).
[60]L. Leuzzi and G. Parisi, J. Stat. Phys. **103**, 679 (2001).
[61]If $J_0 = 0$ we are in the completely disordered case $R_J = \infty$ (also realizable by means of a finite J_0 and $\sigma_J^2 = \infty$). In Ref. 46, $\mathcal{P}$ has been defined as $\sqrt{\beta k_B T_{\rm bath}}$, simply amounting to an adimensional rescaling $\mathcal{P} \to \mathcal{P}\sqrt{J_0 \beta_{\rm bath}}$ with respect to our model case.
[62]L. Angelani, C. Conti, L. Prignano, G. Ruocco, and F. Zamponi, Phys. Rev. B **76**, 064202 (2007).
[63]A. Gordon and B. Fischer, Opt. Commun. **223**, 151 (2003).
[64]A factor of 8 has to be considered because of the overcounting of terms in the Hamiltonian of the model studied in Ref. 45 with respect to Eq. (13). This factor can be absorbed into the temperature yielding the pumping threshold $\mathcal{P}_{\rm PML} = \sqrt{8/T_0}$. If we insert $T_0 \cong 0.717$, i.e., the temperature at which the FM phase first appears in complete absence of disorder, we obtain $\mathcal{P}_{\rm PML} \cong 3.34$. This also exactly corresponds to the spinodal value of $\mathcal{P} = 3.3412$ for $J_0/\sigma_J \to \infty$ in the present model.
[65]J.-L. Barrat, J.-N. Roux, and J.-P. Hansen, Chem. Phys. **149**, 197 (1990).
[66]J.-P. Hasen and S. Yip, Transp. Theory Stat. Phys. **24**, 1149 (1995).
[67]W. Kob and H. C. Andersen, Phys. Rev. Lett. **73**, 1376 (1994).
[68]W. Kob and H. C. Andersen, Phys. Rev. E **51**, 4626 (1995).
[69]W. Kob and H. C. Andersen, Phys. Rev. E **52**, 4134 (1995).
[70]F. Sciortino, W. Kob, and P. Tartaglia, Phys. Rev. Lett. **83**, 3214 (1999).
[71]M. Mézard and G. Parisi, Phys. Rev. Lett. **82**, 747 (1999).
[72]B. Coluzzi, G. Parisi, and P. Verrocchio, Phys. Rev. Lett. **84**, 306 (2000).
[73]E. Marinari, G. Parisi, and F. Ritort, J. Phys. A **27**, 7615 (1994).
[74]E. Marinari, G. Parisi, and F. Ritort, J. Phys. A **27**, 7647 (1994).
[75]L. Cugliandolo, J. Kurchan, and G. Parisi, Phys. Rev. Lett. **74**, 1012 (1995).
[76]D. Sherrington and S. Kirkpatrick, Phys. Rev. Lett. **35**, 1792 (1975).
[77]G. Parisi, Phys. Rev. Lett. **43**, 1754 (1979).
[78]G. Parisi, J. Phys. A **13**, L115 (1980).
[79]M. Mézard, G. Parisi, and M. A. Virasoro, *Spin Glass Theory and Beyond* (World Scientific, Singapore, 1987).
[80]M. Mézard, G. Parisi, and M. Virasoro, Europhys. Lett. **1**, 77 (1986).
[81]F. Guerra, Commun. Math. Phys. **233**, 1 (2003).
[82]M. Talagrand, Ann. Math. **163**, 221 (2006).
[83]M. Mézard, G. Parisi, N. Sourlas, G. Toulouse, and M. Virasoro, Phys. Rev. Lett. **52**, 1156 (1984).
[84]T. Castellani and A. Cavagna, J. Stat. Mech. (2005) P05012.
[85]L. Leuzzi and T. Nieuwenhuizen, *Thermodynamic of the Glassy State* (Taylor & Francis, London, 2007).
[86]E. Gardner, Nucl. Phys. B **257**, 747 (1985).
[87]A. Crisanti and H.-J. Sommers, Z. Phys. B **87**, 341 (1992).
[88]Since in our model the dynamic variables are continuous phases, the whole low-T phase is consistently described by the 1RSB solution, unlike models with discrete variables such as the Ising p-spin model[86] where a further transition occurs at the so-called Gardner temperature.
[89]Technically speaking, this is due to the fact that all the terms of the free energy functional depending on two-index [Q. P. Ehrenfest, Proc. R. Acad. Amsterdam **36**, 154 (1933)] observables have $n - 1$ or $n - m$ factors in front, cf. the Appendix, and in the $n \to 0$ limit these factors change.
[90]The very existence of a Kauzmann temperature, also called the *ideal glass transition temperature*, in structural glasses is, actually, a matter of debate.
[91]The paramagnetic phase exists as metastable also at $T < T_s$, but the phase space is disconnected and the ergodicity is broken because of infinite barriers.
[92]D. Thouless, P. Anderson, and R. Palmer, Philos. Mag. **35**, 593 (1977).
[93]A. J. Bray and M. A. Moore, J. Phys. C **13**, L469 (1980).
[94]A. Crisanti, L. Leuzzi, G. Parisi, and T. Rizzo, Phys. Rev. B **68**, 174401 (2003).
[95]A. Crisanti, L. Leuzzi, and T. Rizzo, Eur. Phys. J. B **36**, 129 (2003).
[96]A. Annibale, A. Cavagna, I. Giardina, and G. Parisi, J. Phys. A **36**, 10937 (2003).
[97]A. Crisanti, L. Leuzzi, G. Parisi, and T. Rizzo, Phys. Rev. B **70**, 064423 (2004).
[98]A. Crisanti, L. Leuzzi, G. Parisi, and T. Rizzo, Phys. Rev. Lett. **92**, 127203 (2004).
[99]T. Aspelmeier, A. J. Bray, and M. A. Moore, Phys. Rev. Lett. **92**, 087203 (2004).
[100] A. Crisanti, L. Leuzzi, and T. Rizzo, Phys. Rev. B **71**, 094202 (2005).
[101] M. Müller, L. Leuzzi, and A. Crisanti, Phys. Rev. B **74**, 134431 (2006).
[102] S. Edwards and P. Anderson, J. Phys. F **5**, 965 (1975).
[103] A. Gordon and B. Fischer, Phys. Rev. Lett. **89**, 103901 (2002).
[104] P. Ehrenfest, Proc. R. Acad. Amsterdam **36**, 154 (1980).
[105]The case at $J_0 = 0$ was explicitly considered in Ref. 45.